

APPENDIX A SNOWMELT DISCHARGE CLIMATOLOGY

The long-term mean (climatology) of river discharge.

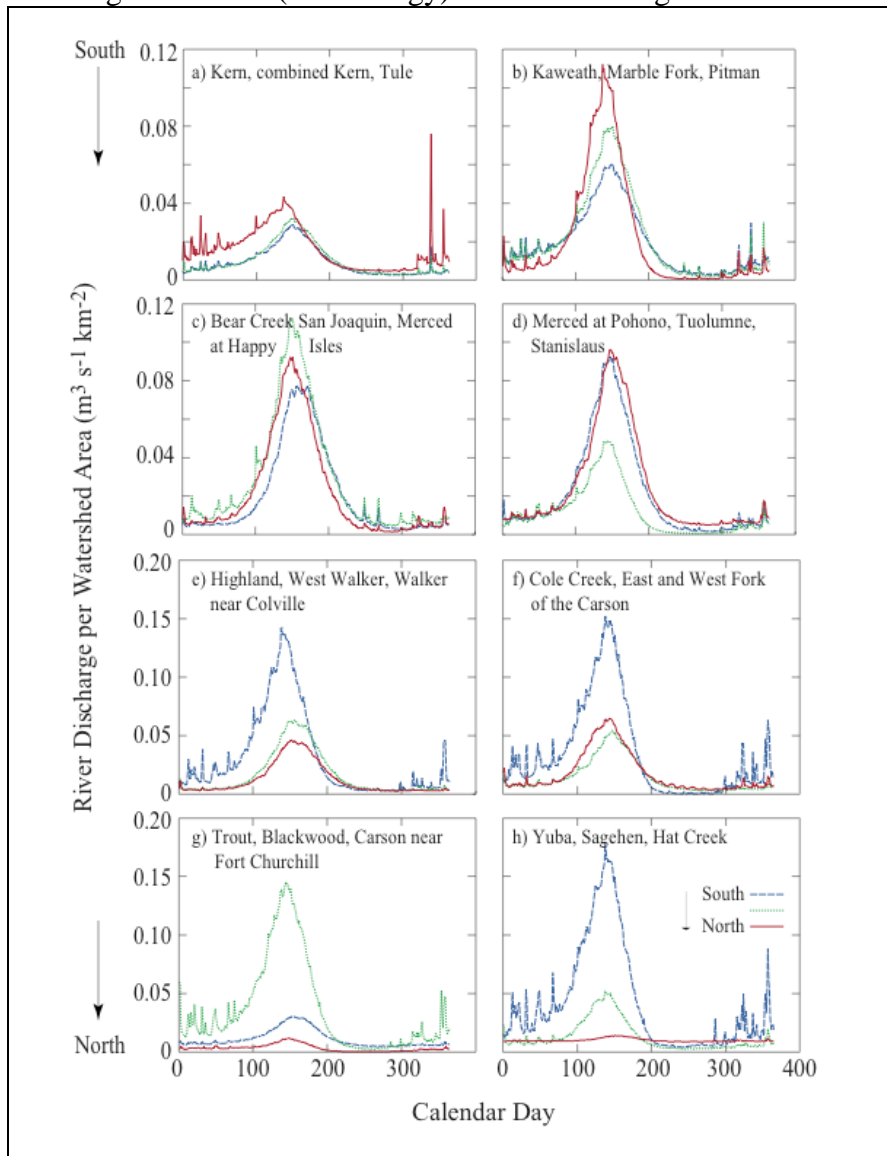


Fig. A. Long-term daily mean of river discharge for the rivers and creeks in Fig. 1: a) Kern, combined Kern, and Tule; b) Kaweah, Marble Fork, and Pitman; c) Bear Creek, San Joaquin and Merced at Happy Isles; d) Merced at Pohono, Tuolumne, and Stanislaus; e) Highland, West Walker, and Walker near Colville; f) Cole Creek, East and West Fork of the Carson; g) Trout, Blackwood and Carson near Fort Churchill; h) Yuba, Sagehen, and Hat Creek. The order of presentation is from south to north along the Sierra Nevada and the spatial/color order for the three rivers or creeks in the panels is blue, green and red. Note the change in vertical scaling between the top 12 watersheds to the south compared to the 12 to the north. Further, low base flow watersheds, especially Pitman and Cole Creeks, show a quick decline towards base flow following peak flow, whereas the watersheds with higher base flow generally do not.

APPENDIX B TRENDS IN EARLY SNOWMELT

The individual trends in early snowmelt based on estimates of the timing of the start of the spring pulse (red) and timing of the center of mass (blue).

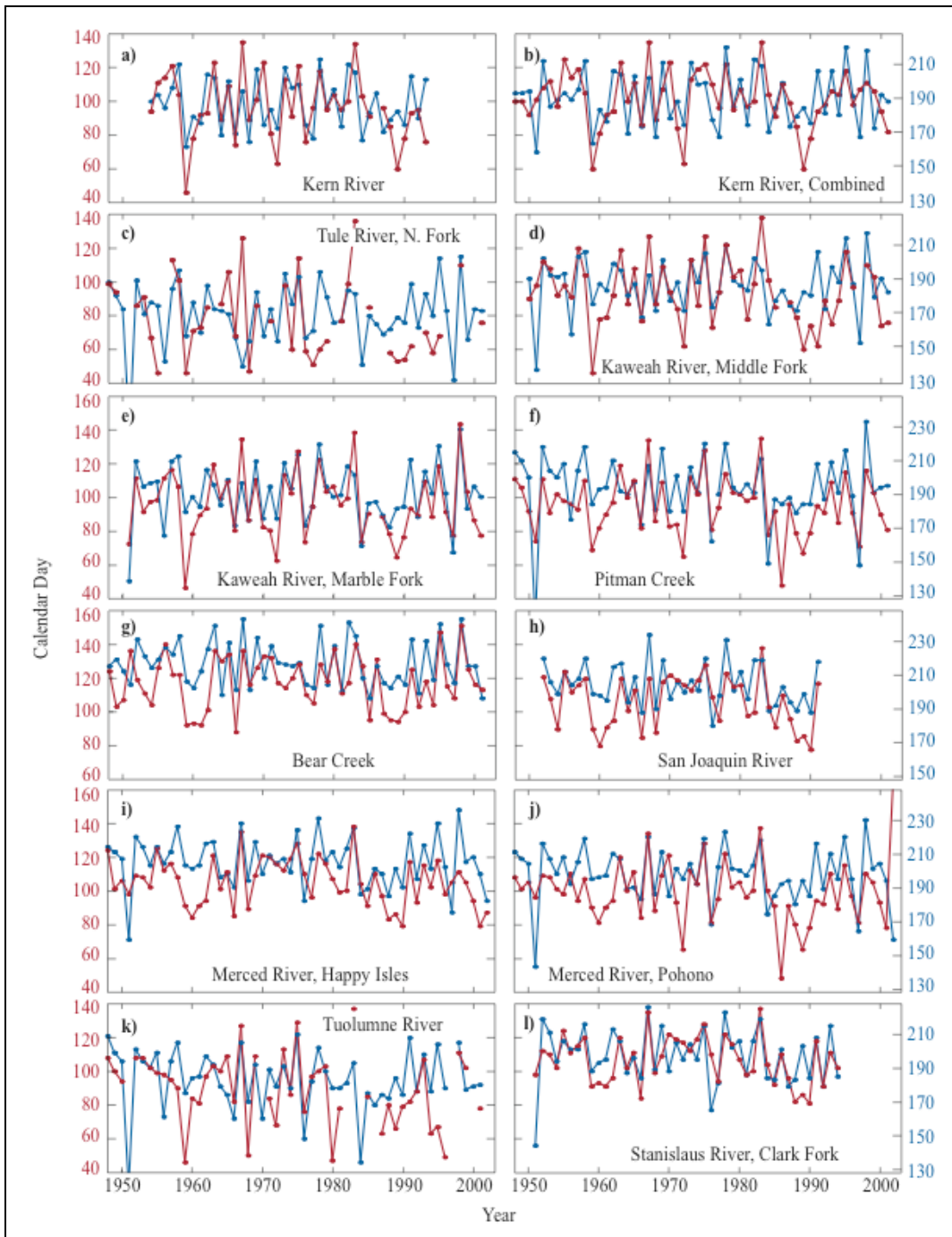


Fig. B1. Trends in timing of the spring pulse (red) and center of mass (blue) for the 12 watersheds in the southern Sierra Nevada. Note the importance of time series length and timing. For example, the Kern (a) compared to the combined Kern (b). Also, in an early timing in 1959 compared to the late timing in 1967 was due to an approximately 10 degree difference in air temperature with almost a 100 day difference in timing, or roughly, 10 days earlier per 1 degree rise in air temperature.

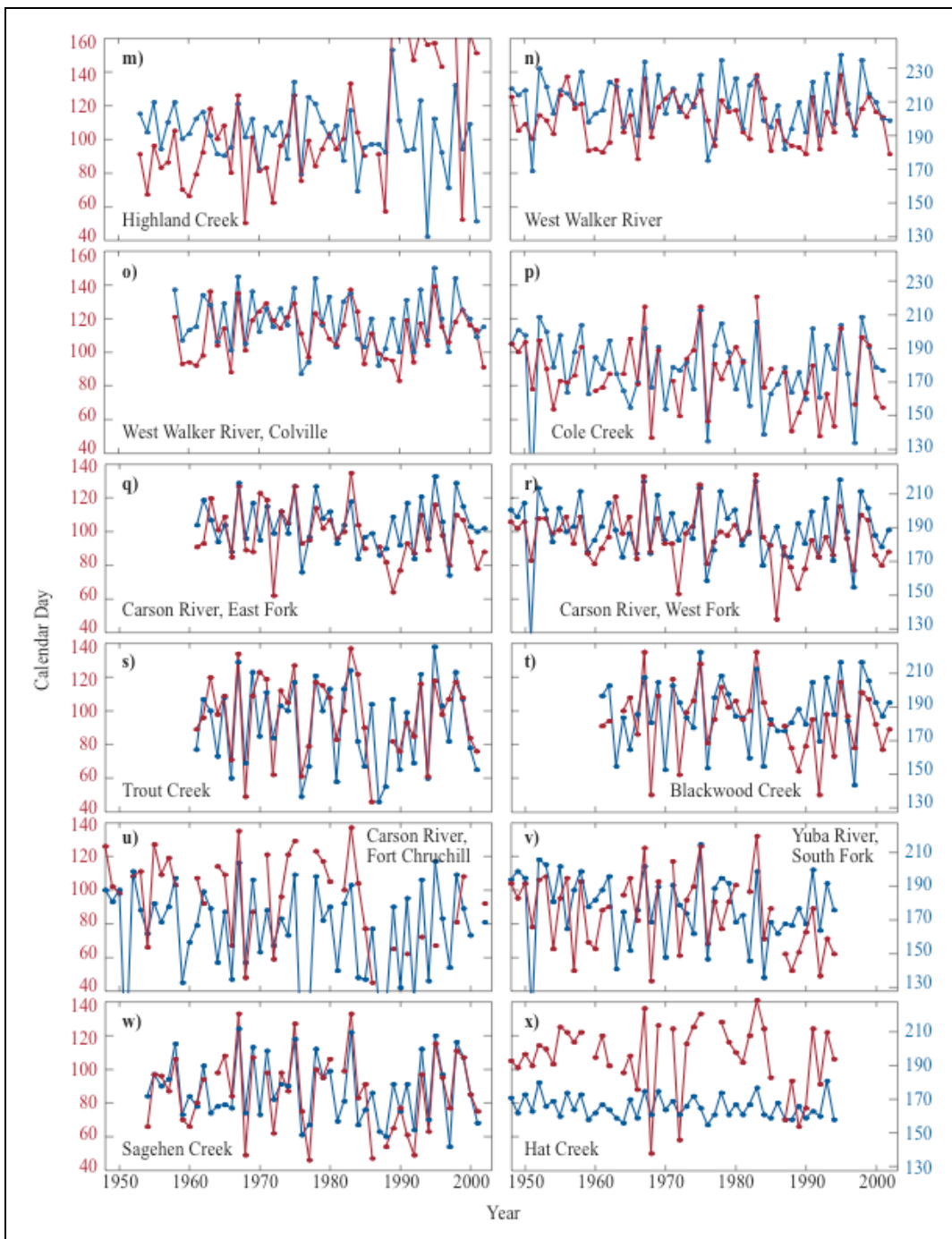


Fig. B2. Trends in timing of the spring pulse (red) and center of mass (blue) for the 12 watersheds in the northern Sierra Nevada. Some of the sources of variability include the following: The center of mass is earlier in years with large winter floods (i.e., 1951); differences in record length (i.e., the slope of the trend increases if the time series ends in the early to mid 1990s, such as for the south fork of the Yuba River); human influences (i.e., Highland Creek after 1988 and the Carson River at Fort Churchill); results in years with wet winters and cool springs show similar responses for the two methods (i.e., 1967, 1975 and 1983).

APPENDIX C INTERBASIN PEAK/BASE FLOW PREDICTION

The plots in this appendix are peak and base flow values from the 23 watersheds, compared to the Merced River at Happy Isles peak and base flow, with respect to increasing mean annual snowmelt runoff. Although the comparison is straight forward, a generalization of the comparison procedure is given. The response of peak or base flow runoff with respect to increasing mean annual runoff is always positive (i.e., both peak and base flow increase in wet versus dry years). However, comparison of basin to basin differences in the peak and base flow responses show if the rate of increase in peak flow in basin A is greater than basin B, then the rate of increase in base flow in basin B is generally greater than basin A (over a range in runoff). Thus, if the slope of the difference in peak response in basin B minus A is a negative increase, basin A had the stronger peak response (conceptually basin A has a “thinner” soil response). Then, if the same difference is made, basin B minus basin A, but for base flow, the response is less for basin A than B and the result is a positive increase (conceptually basin B has a “thicker” soil response). These reversals were observed in 17 out of the 24 gage comparisons, with some plots very noisy. Also a stronger base flow response infers greater soil water storage.

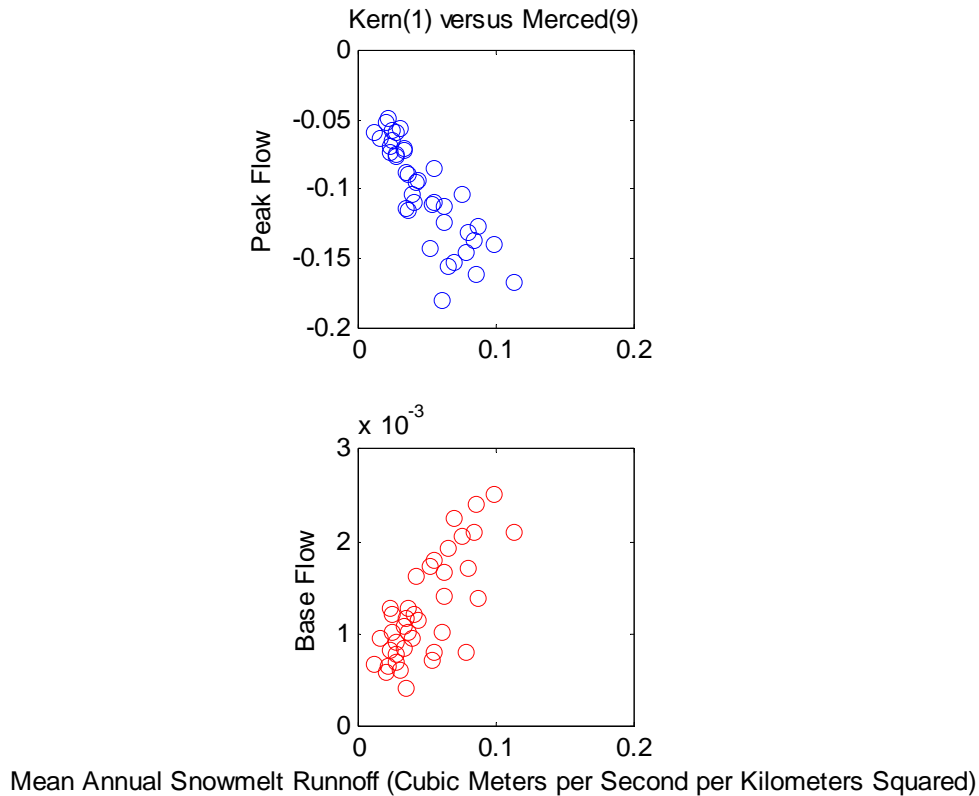


Fig. C1. Upper panel, the vertical axis is the peak flow (runoff) of the Kern River at Kernville with respect to the mean annual snowmelt runoff of the Merced River at Happy Isles minus the peak flow (runoff) of the Merced River at Happy Isles with respect to the mean annual snowmelt runoff of the Merced River at Happy Isles. The horizontal axis is the mean annual snowmelt runoff of the Merced River at Happy Isles ($R=-0.85$). Lower panel, the axes are the same as the upper panel, but for base flow ($R=0.75$).

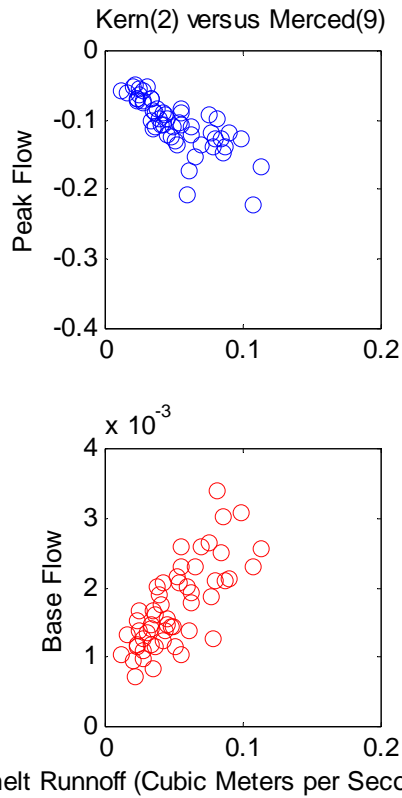


Fig. C2. Upper panel, the vertical axis is the peak flow (runoff) of the Combined Kern River with respect to the mean annual snowmelt runoff of the Merced River at Happy Isles minus the peak flow (runoff) of the Merced River at Happy Isles with respect to the mean annual snowmelt runoff of the Merced River at Happy Isles. The horizontal axis is the mean annual snowmelt runoff of the Merced River at Happy Isles ($R=-0.77$). Lower panel, the axes are the same as the upper panel, but for base flow ($R=0.75$).

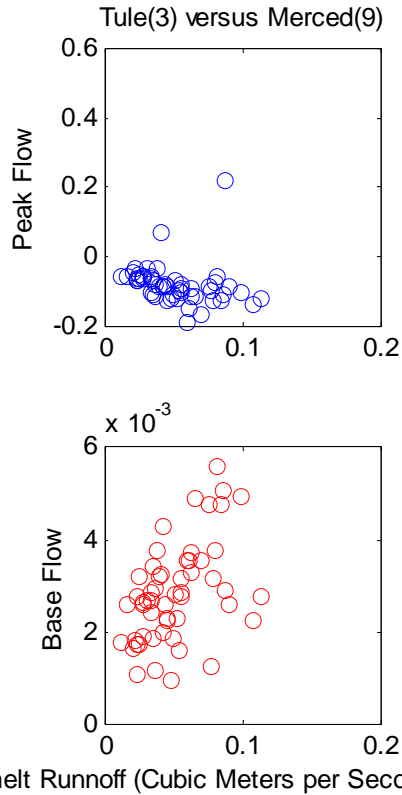


Fig. C3. Upper panel, the vertical axis is the peak flow (runoff) of the Tule River with respect to the mean annual snowmelt runoff of the Merced River at Happy Isles minus the peak flow (runoff) of the Merced River at Happy Isles with respect to the mean annual snowmelt runoff of the Merced River at Happy Isles. The horizontal axis is the mean annual snowmelt runoff of the Merced River at Happy Isles ($R=-0.18$). Lower panel, the axes are the same as the upper panel, but for base flow ($R=0.48$).

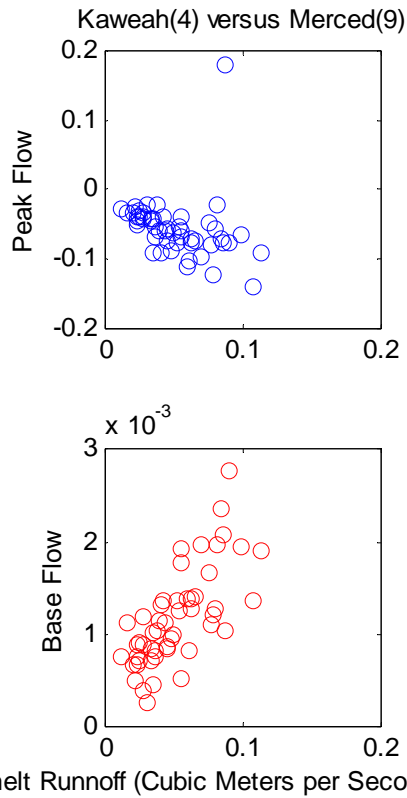


Fig. C4. Upper panel, the vertical axis is the peak flow (runoff) of the Middle Fork of the Kaweah River with respect to the mean annual snowmelt runoff of the Merced River at Happy Isles minus the peak flow (runoff) of the Merced River at Happy Isles with respect to the mean annual snowmelt runoff of the Merced River at Happy Isles. The horizontal axis is the mean annual snowmelt runoff of the Merced River at Happy Isles ($R=-0.21$). Lower panel, the axes are the same as the upper panel, but for base flow ($R=0.75$).

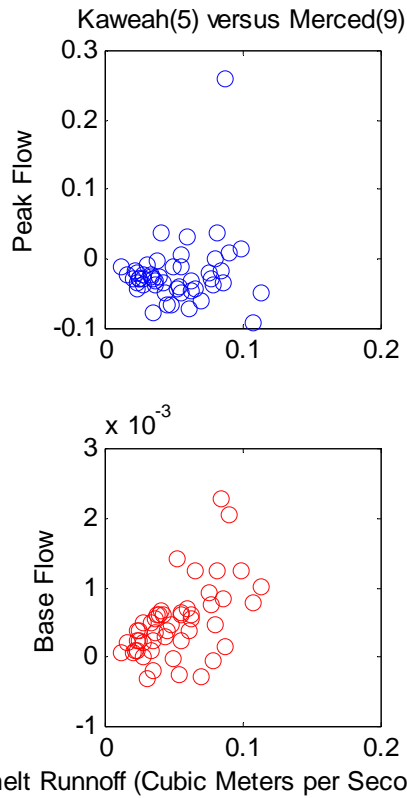


Fig. C5. Upper panel, the vertical axis is the peak flow (runoff) of the Marble Fork of the Kaweah River with respect to the mean annual snowmelt runoff of the Merced River at Happy Isles minus the peak flow (runoff) of the Merced River at Happy Isles with respect to the mean annual snowmelt runoff of the Merced River at Happy Isles. The horizontal axis is the mean annual snowmelt runoff of the Merced River at Happy Isles ($R=-0.17$). Lower panel, the axes are the same as the upper panel, but for base flow ($R=0.55$).

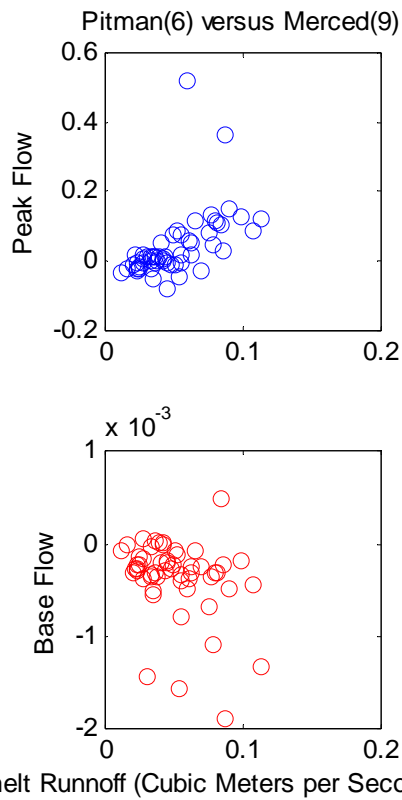


Fig. C6. Upper panel, the vertical axis is the peak flow (runoff) of the Pitman Creek with respect to the mean annual snowmelt runoff of the Merced River at Happy Isles minus the peak flow (runoff) of the Merced River at Happy Isles with respect to the mean annual snowmelt runoff of the Merced River at Happy Isles. The horizontal axis is the mean annual snowmelt runoff of the Merced River at Happy Isles ($R=0.54$). Lower panel, the axes are the same as the upper panel, but for base flow ($R=-0.31$).

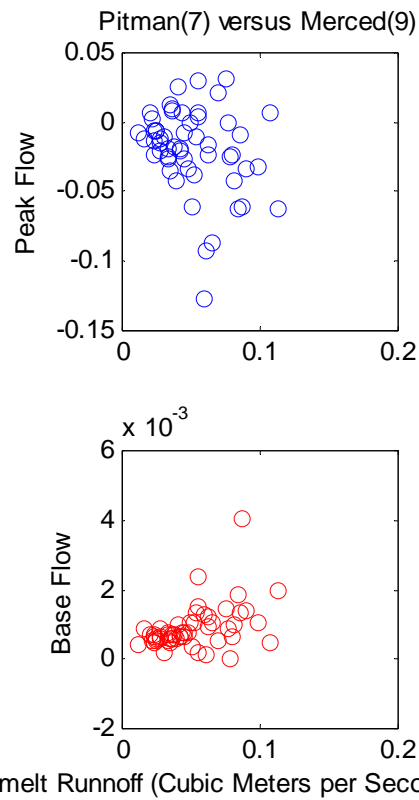


Fig. C7. Upper panel, the vertical axis is the peak flow (runoff) of the Bear Creek with respect to the mean annual snowmelt runoff of the Merced River at Happy Isles minus the peak flow (runoff) of the Merced River at Happy Isles with respect to the mean annual snowmelt runoff of the Merced River at Happy Isles. The horizontal axis is the mean annual snowmelt runoff of the Merced River at Happy Isles ($R=-0.27$). Lower panel, the axes are the same as the upper panel, but for base flow ($R=0.45$).

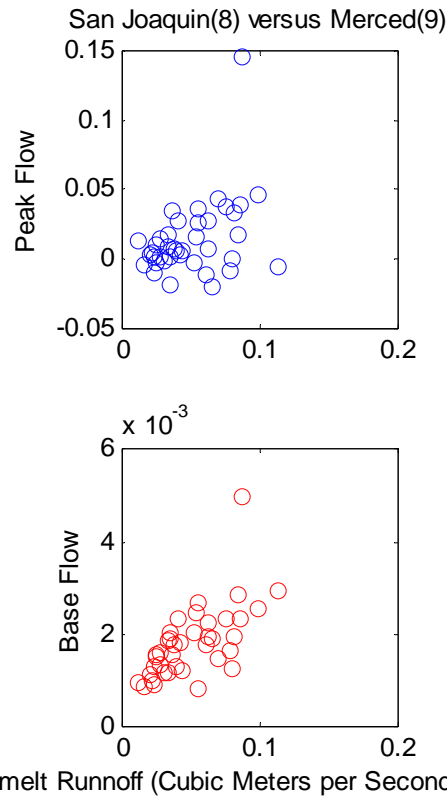


Fig. C8. Upper panel, the vertical axis is the peak flow (runoff) of the San Joaquin River with respect to the mean annual snowmelt runoff of the Merced River at Happy Isles minus the peak flow (runoff) of the Merced River at Happy Isles with respect to the mean annual snowmelt runoff of the Merced River at Happy Isles. The horizontal axis is the mean annual snowmelt runoff of the Merced River at Happy Isles ($R=0.39$). Lower panel, the axes are the same as the upper panel, but for base flow ($R=0.65$).

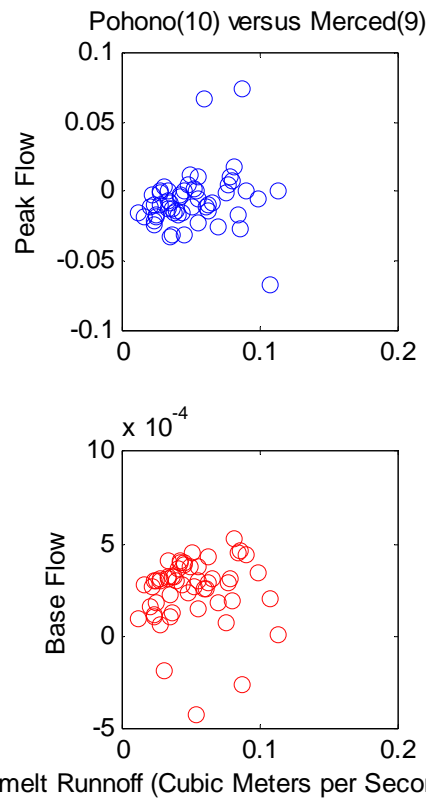


Fig. C9. Upper panel, the vertical axis is the peak flow (runoff) of the Merced River at Pohono with respect to the mean annual snowmelt runoff of the Merced River at Happy Isles minus the peak flow (runoff) of the Merced River at Happy Isles with respect to the mean annual snowmelt runoff of the Merced River at Happy Isles. The horizontal axis is the mean annual snowmelt runoff of the Merced River at Happy Isles ($R=-0.16$). Lower panel, the axes are the same as the upper panel, but for base flow ($R=0.05$).

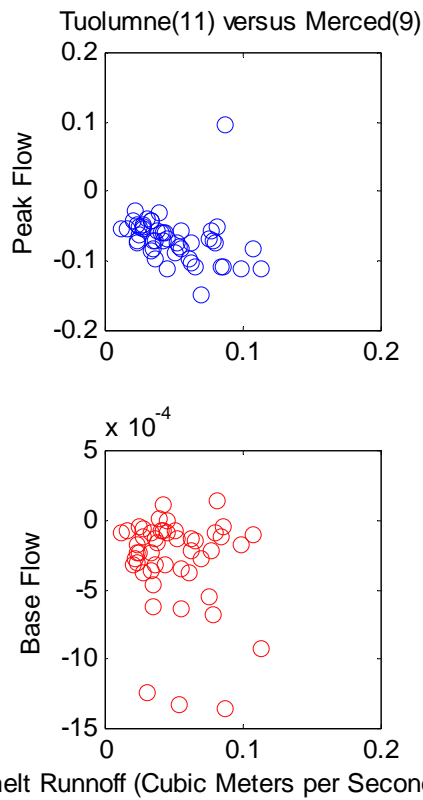


Fig. C10. Upper panel, the vertical axis is the peak flow (runoff) of the Tuolumne River with respect to the mean annual snowmelt runoff of the Merced River at Happy Isles minus the peak flow (runoff) of the Merced River at Happy Isles with respect to the mean annual snowmelt runoff of the Merced River at Happy Isles. The horizontal axis is the mean annual snowmelt runoff of the Merced River at Happy Isles ($R=-0.26$). Lower panel, the axes are the same as the upper panel, but for base flow ($R=-0.18$).

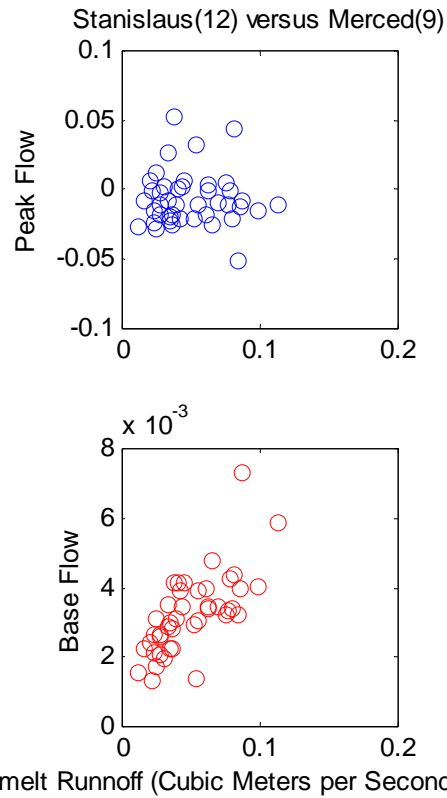


Fig. C11. Upper panel, the vertical axis is the peak flow (runoff) of the Stanislaus River with respect to the mean annual snowmelt runoff of the Merced River at Happy Isles minus the peak flow (runoff) of the Merced River at Happy Isles with respect to the mean annual snowmelt runoff of the Merced River at Happy Isles. The horizontal axis is the mean annual snowmelt runoff of the Merced River at Happy Isles ($R=-0.02$). Lower panel, the axes are the same as the upper panel, but for base flow ($R=0.70$).

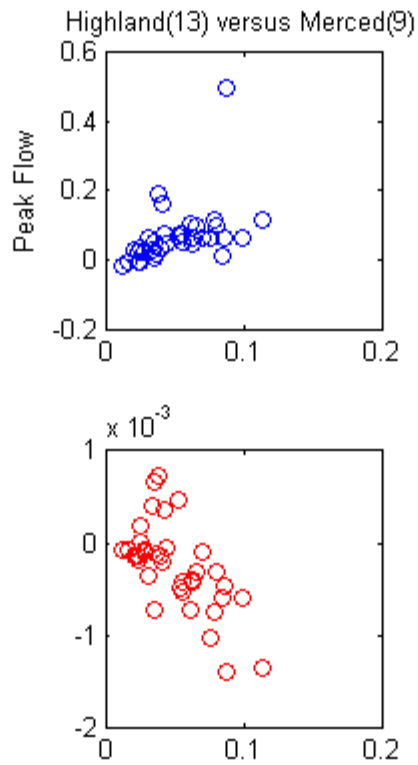


Fig. C12. Upper panel, the vertical axis is the peak flow (runoff) of the Highland Creek River with respect to the mean annual snowmelt runoff of the Merced River at Happy Isles minus the peak flow (runoff) of the Merced River at Happy Isles with respect to the mean annual snowmelt runoff of the Merced River at Happy Isles. The horizontal axis is the mean annual snowmelt runoff of the Merced River at Happy Isles ($R=0.46$). Lower panel, the axes are the same as the upper panel, but for base flow ($R=-0.65$).

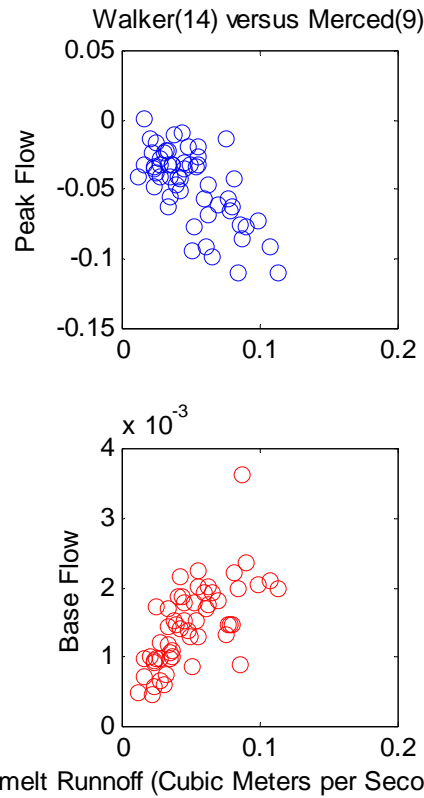


Fig. C13. Upper panel, the vertical axis is the peak flow (runoff) of the West Walker River with respect to the mean annual snowmelt runoff of the Merced River at Happy Isles minus the peak flow (runoff) of the Merced River at Happy Isles with respect to the mean annual snowmelt runoff of the Merced River at Happy Isles. The horizontal axis is the mean annual snowmelt runoff of the Merced River at Happy Isles ($R=-0.68$). Lower panel, the axes are the same as the upper panel, but for base flow ($R=0.66$).

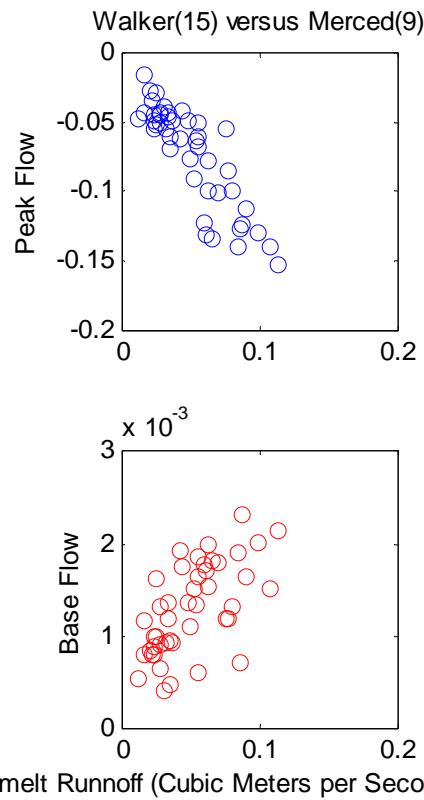


Fig. C14. Upper panel, the vertical axis is the peak flow (runoff) of the West Walker River at Coleville with respect to the mean annual snowmelt runoff of the Merced River at Happy Isles minus the peak flow (runoff) of the Merced River at Happy Isles with respect to the mean annual snowmelt runoff of the Merced River at Happy Isles. The horizontal axis is the mean annual snowmelt runoff of the Merced River at Happy Isles ($R=-0.87$). Lower panel, the axes are the same as the upper panel, but for base flow ($R=0.63$).

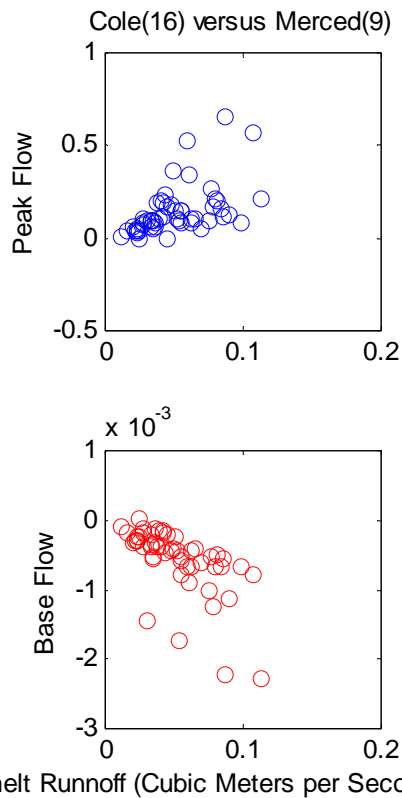


Fig. C15. Upper panel, the vertical axis is the peak flow (runoff) of the Cole Creek River with respect to the mean annual snowmelt runoff of the Merced River at Happy Isles minus the peak flow (runoff) of the Merced River at Happy Isles with respect to the mean annual snowmelt runoff of the Merced River at Happy Isles. The horizontal axis is the mean annual snowmelt runoff of the Merced River at Happy Isles ($R=0.53$). Lower panel, the axes are the same as the upper panel, but for base flow ($R=-0.63$).

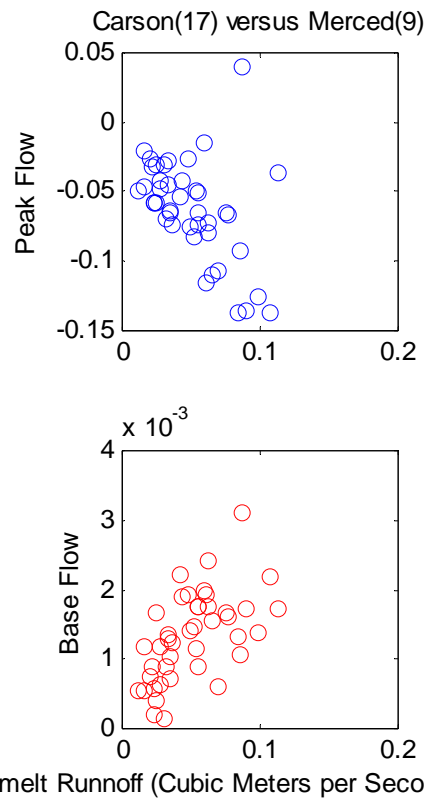


Fig. C16. Upper panel, the vertical axis is the peak flow (runoff) of the East Fork of the Carson River with respect to the mean annual snowmelt runoff of the Merced River at Happy Isles minus the peak flow (runoff) of the Merced River at Happy Isles with respect to the mean annual snowmelt runoff of the Merced River at Happy Isles. The horizontal axis is the mean annual snowmelt runoff of the Merced River at Happy Isles ($R=-0.47$). Lower panel, the axes are the same as the upper panel, but for base flow ($R=0.58$).

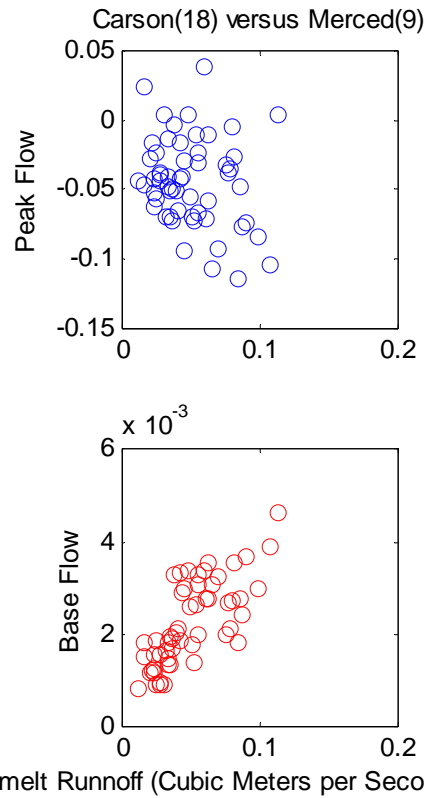
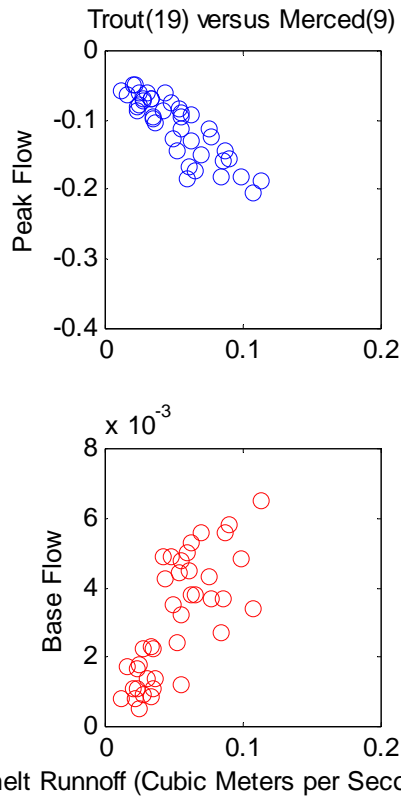


Fig. C17. Upper panel, the vertical axis is the peak flow (runoff) of the West Fork of the Carson River with respect to the mean annual snowmelt runoff of the Merced River at Happy Isles minus the peak flow (runoff) of the Merced River at Happy Isles with respect to the mean annual snowmelt runoff of the Merced River at Happy Isles. The horizontal axis is the mean annual snowmelt runoff of the Merced River at Happy Isles ($R=-0.22$). Lower panel, the axes are the same as the upper panel, but for base flow ($R=0.73$).



Mean Annual Snowmelt Runoff (Cubic Meters per Second per Kilometers Squared)

Fig. C18. Upper panel, the vertical axis is the peak flow (runoff) of the Trout Creek with respect to the mean annual snowmelt runoff of the Merced River at Happy Isles minus the peak flow (runoff) of the Merced River at Happy Isles with respect to the mean annual snowmelt runoff of the Merced River at Happy Isles. The horizontal axis is the mean annual snowmelt runoff of the Merced River at Happy Isles ($R=-0.86$). Lower panel, the axes are the same as the upper panel, but for base flow ($R=0.75$).

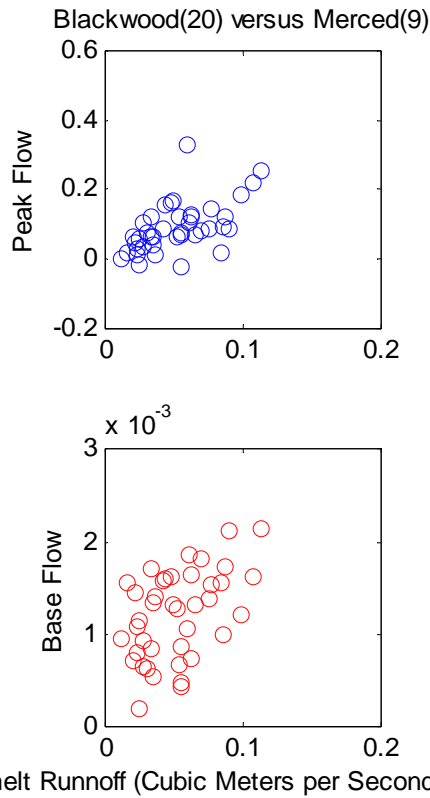


Fig. C19. Upper panel, the vertical axis is the peak flow (runoff) of the Blackwood Creek with respect to the mean annual snowmelt runoff of the Merced River at Happy Isles minus the peak flow (runoff) of the Merced River at Happy Isles with respect to the mean annual snowmelt runoff of the Merced River at Happy Isles. The horizontal axis is the mean annual snowmelt runoff of the Merced River at Happy Isles ($R=0.57$). Lower panel, the axes are the same as the upper panel, but for base flow ($R=0.48$).

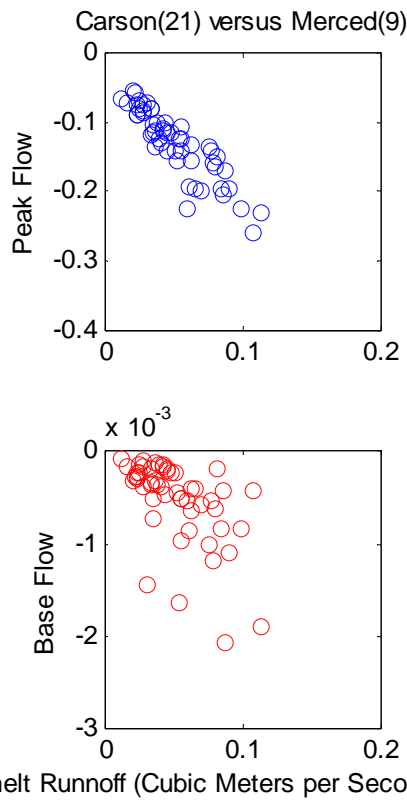


Fig. C20. Upper panel, the vertical axis is the peak flow (runoff) of the Carson River at Churchill with respect to the mean annual snowmelt runoff of the Merced River at Happy Isles minus the peak flow (runoff) of the Merced River at Happy Isles with respect to the mean annual snowmelt runoff of the Merced River at Happy Isles. The horizontal axis is the mean annual snowmelt runoff of the Merced River at Happy Isles ($R=-0.90$). Lower panel, the axes are the same as the upper panel, but for base flow ($R=-0.57$).

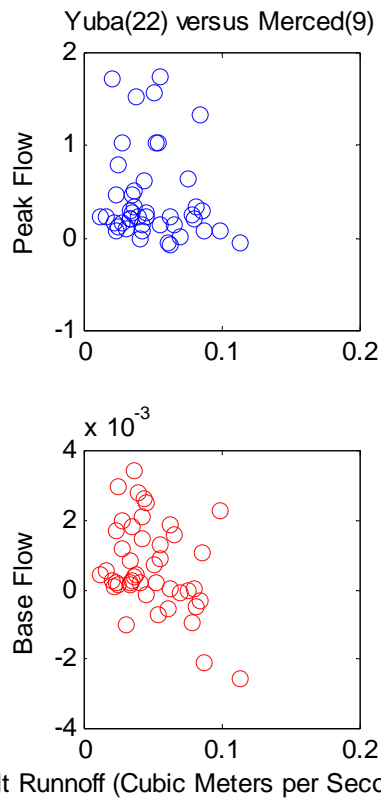


Fig. C21. Upper panel, the vertical axis is the peak flow (runoff) of the Yuba River with respect to the mean annual snowmelt runoff of the Merced River at Happy Isles minus the peak flow (runoff) of the Merced River at Happy Isles with respect to the mean annual snowmelt runoff of the Merced River at Happy Isles. The horizontal axis is the mean annual snowmelt runoff of the Merced River at Happy Isles ($R=-0.12$). Lower panel, the axes are the same as the upper panel, but for base flow ($R=-0.36$).

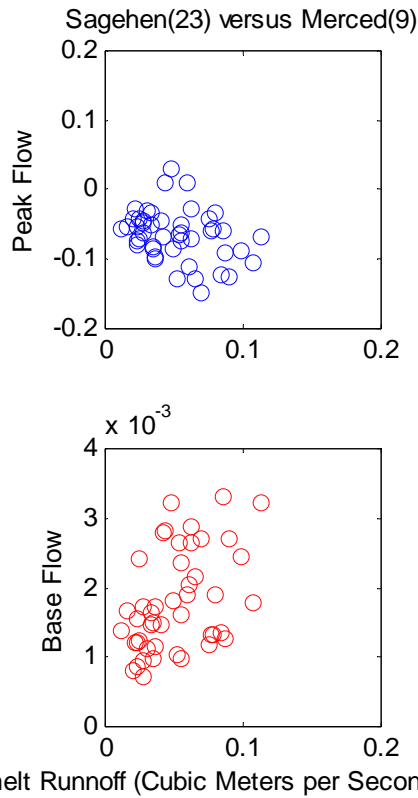


Fig. C22. Upper panel, the vertical axis is the peak flow (runoff) of the Sagehen Creek with respect to the mean annual snowmelt runoff of the Merced River at Happy Isles minus the peak flow (runoff) of the Merced River at Happy Isles with respect to the mean annual snowmelt runoff of the Merced River at Happy Isles ($R=-0.31$). Lower panel, the axes are the same as the upper panel, but for base flow ($R=0.45$).

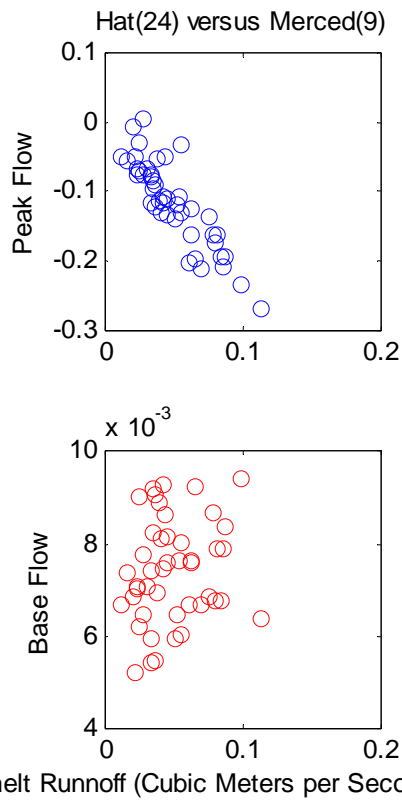


Fig. C23. Upper panel, the vertical axis is the peak flow (runoff) of the Hat Creek with respect to the mean annual snowmelt runoff of the Merced River at Happy Isles minus the peak flow (runoff) of the Merced River at Happy Isles with respect to the mean annual snowmelt runoff of the Merced River at Happy Isles. The horizontal axis is the mean annual snowmelt runoff of the Merced River at Happy Isles ($R=-0.87$). Lower panel, the axes are the same as the upper panel, but for base flow ($R=0.17$).

APPENDIX D PEAK AND BASE FLOW PREDICTION

Peak and base flow magnitude correlations with initial snow water equivalent (SWE).

Least squares (LS) and orthogonal least squares (OLS) regression models are shown in the Figures. For OLS, the closest distance of a point from the line is minimized, forming a ‘orthogonal line’ to the line of regression, while for standard LS only the y-distance of each point from the regression line is minimized. The OLS and the LS should give similar results for the linear case. However, for this study, the results for OLS were typically poor because this method appears to be sensitive to outliers. Note the timing is in relation to increasing SWE and is not a time series (it takes more energy to melt more snow). For plot statistics, intercept, slope and correlation contact Iris Stewart.

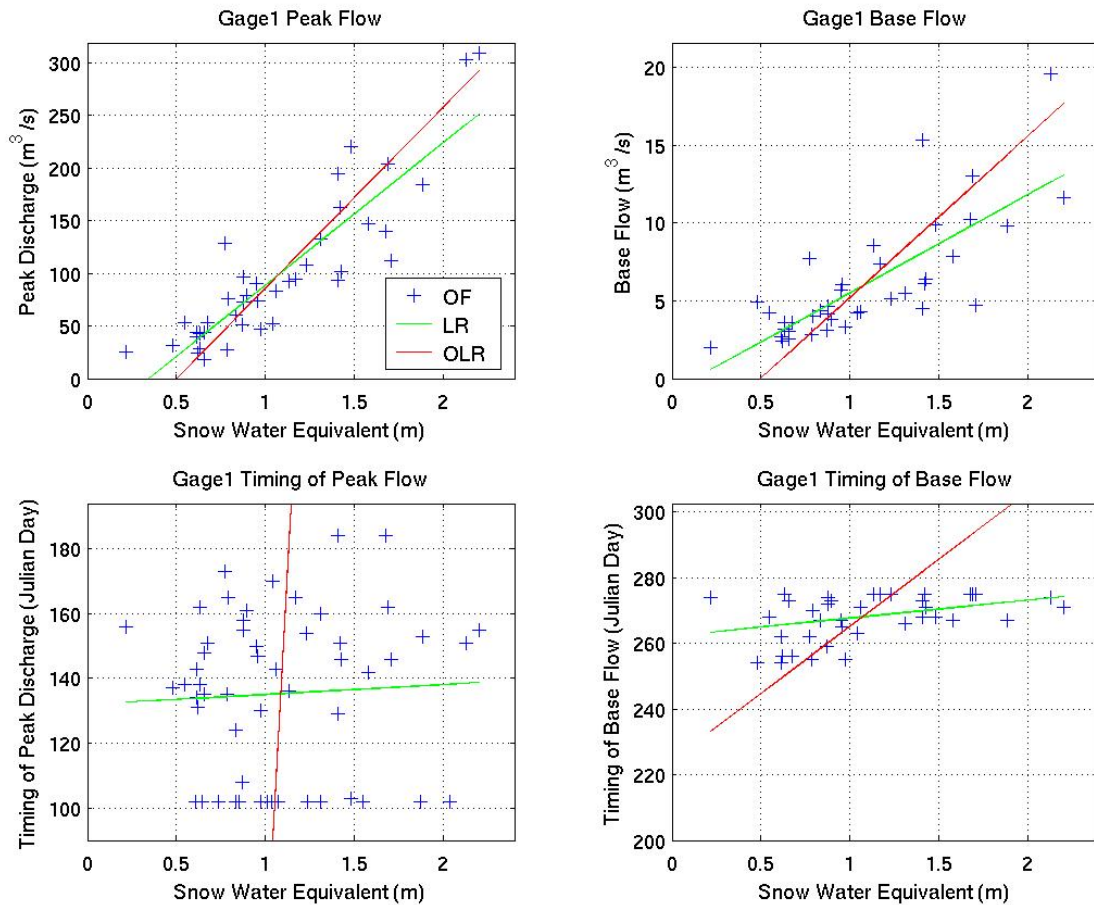


Fig. D1. Kern at Kernville Upper left panel, peak flow as a linear function of snow water equivalent, observed historic values (+), linear least squares regression (green) and orthogonal least squares regression (red); upper right panel, same as upper left panel but for base flow; lower left panel, same as upper left panel but for peak flow timing; and lower right panel, same as upper left panel but for base flow timing.

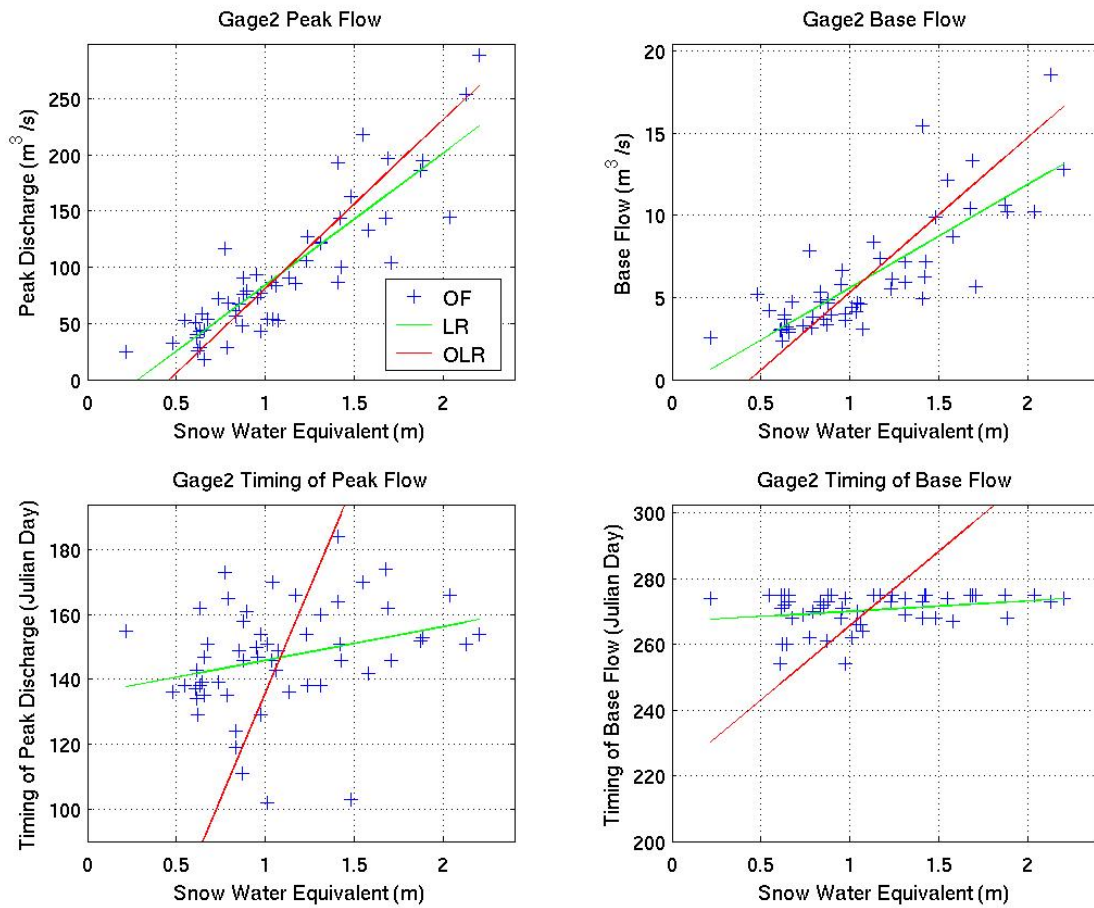


Fig. D2. Combined Kern Upper left panel, peak flow as a linear function of snow water equivalent, observed historic values (+), linear least squares regression (green) and orthogonal least squares regression (red); upper right panel, same as upper left panel but for base flow; lower left panel, same as upper left panel but for peak flow timing; and lower right panel, same as upper left panel but for base flow timing.

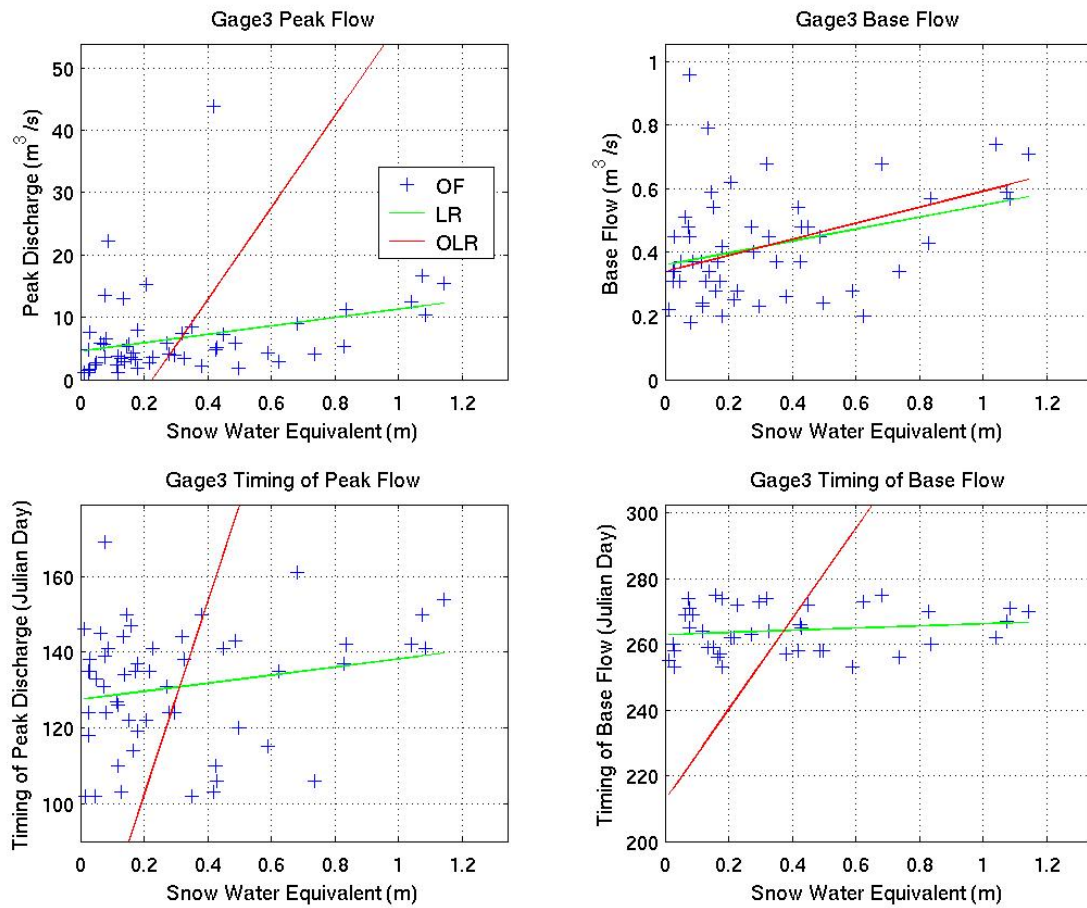


Fig. D3. North Fork Tule Upper left panel, peak flow as a linear function of snow water equivalent, observed historic values (+), linear least squares regression (green) and orthogonal least squares regression (red); upper right panel, same as upper left panel but for base flow; lower left panel, same as upper left panel but for peak flow timing; and lower right panel, same as upper left panel but for base flow timing.

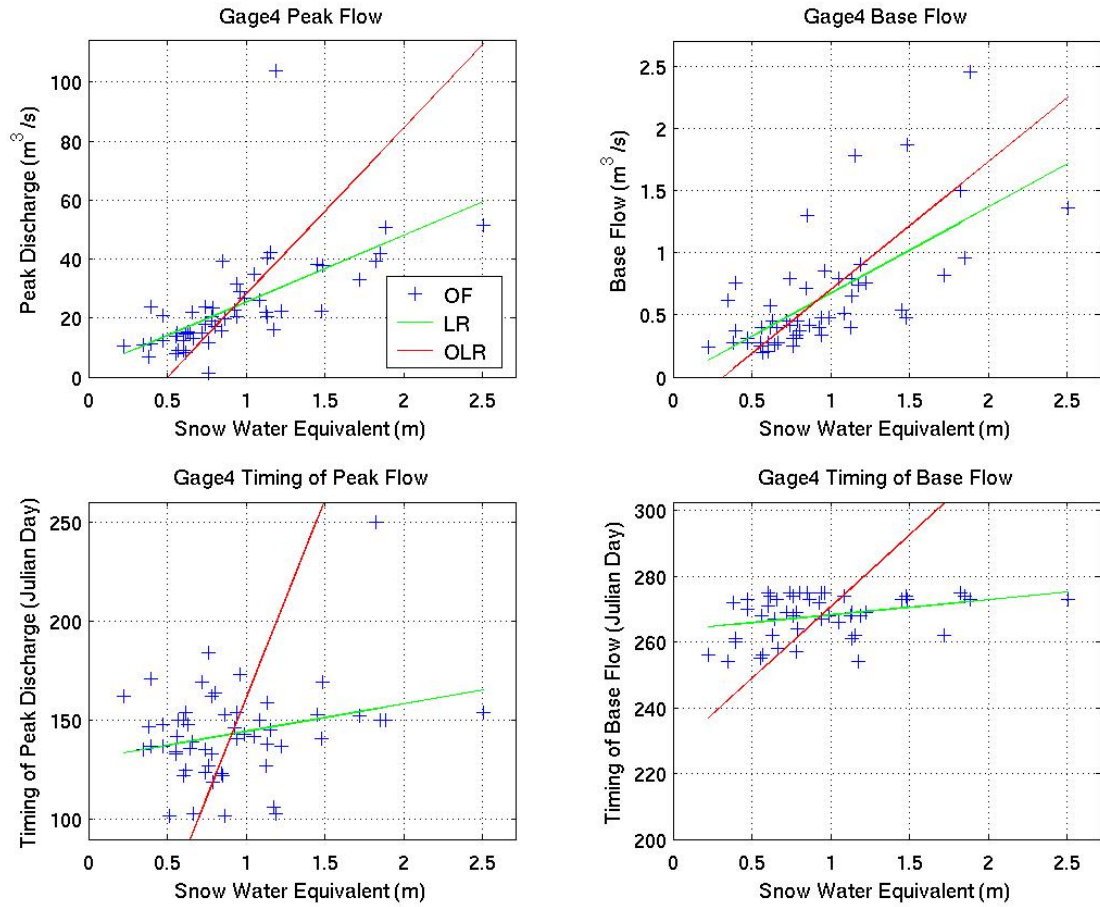


Fig. D4. Middle Fork Kaweah Upper left panel, peak flow as a linear function of snow water equivalent, observed historic values (+), linear least squares regression (green) and orthogonal least squares regression (red); upper right panel, same as upper left panel but for base flow; lower left panel, same as upper left panel but for peak flow timing; and lower right panel, same as upper left panel but for base flow timing.

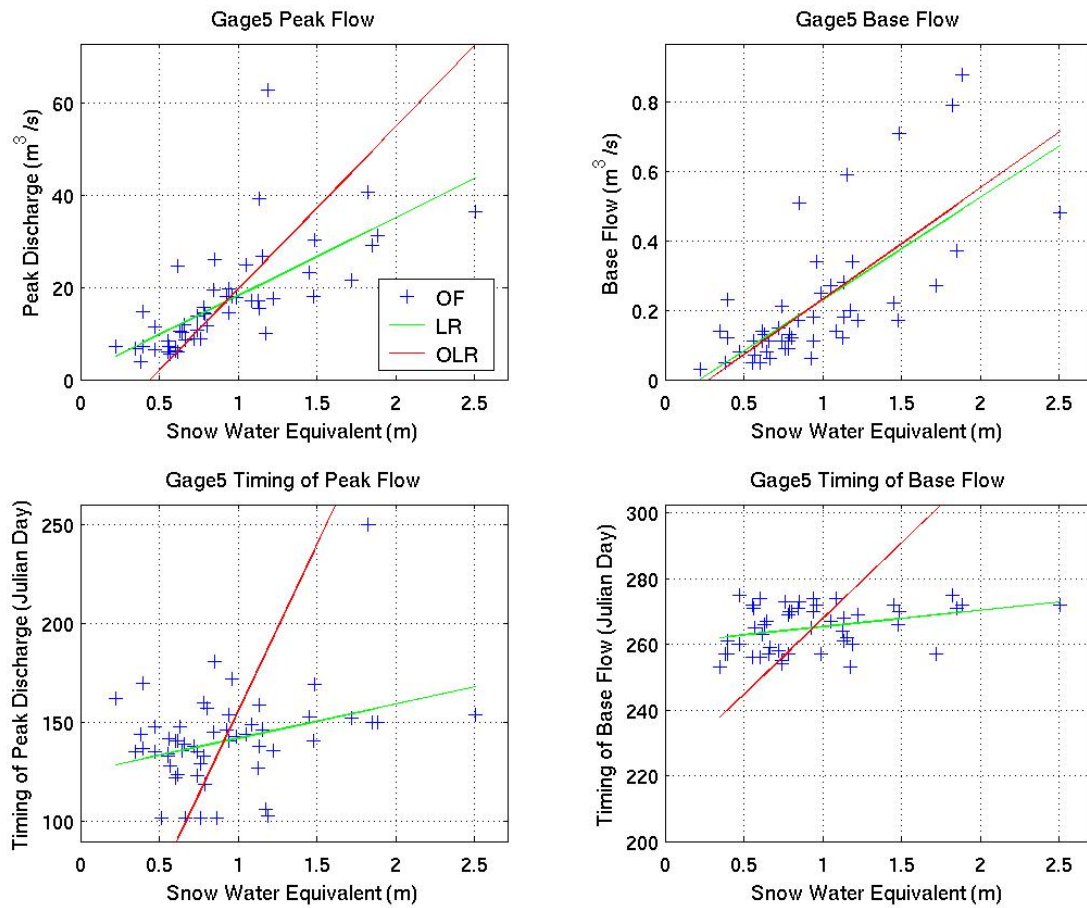


Fig. D5. Marble Fork Kaweah Upper left panel, peak flow as a linear function of snow water equivalent, observed historic values (+), linear least squares regression (green) and orthogonal least squares regression (red); upper right panel, same as upper left panel but for base flow; lower left panel, same as upper left panel but for peak flow timing; and lower right panel, same as upper left panel but for base flow timing.

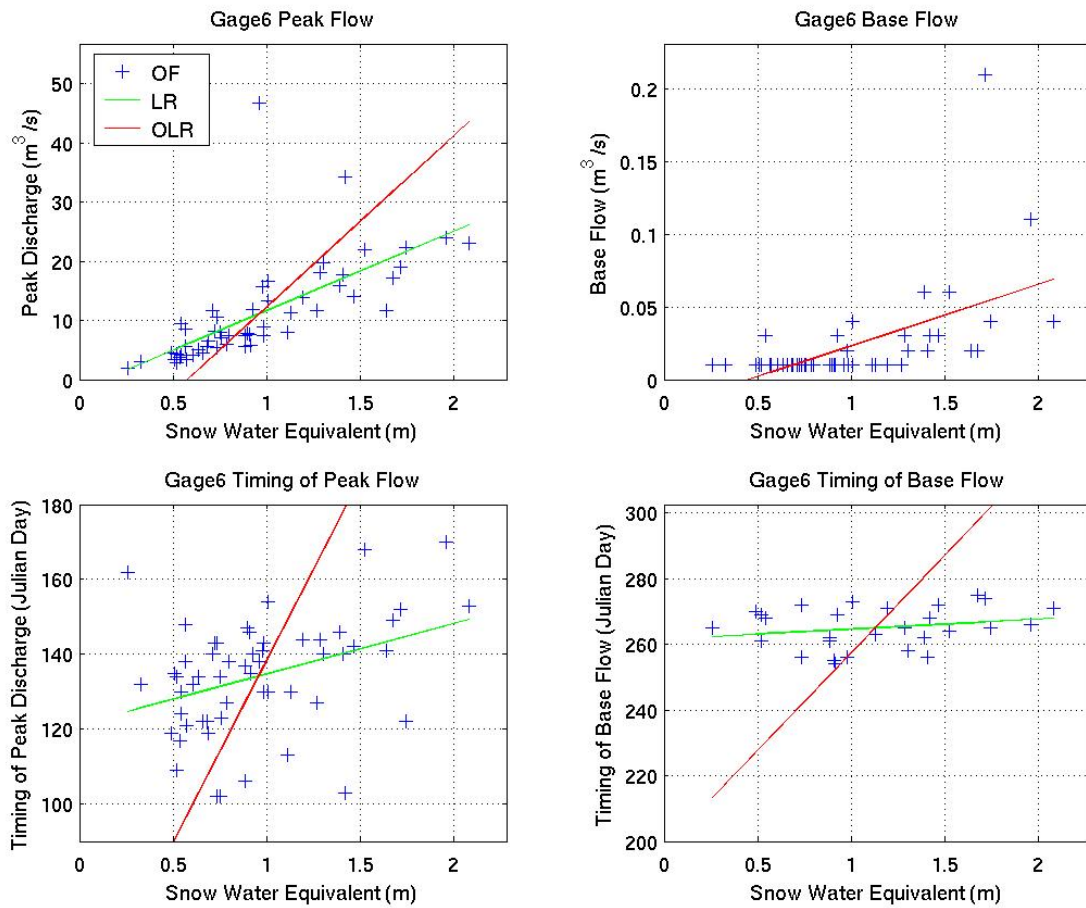


Fig. D6. Pitman Creek Upper left panel, peak flow as a linear function of snow water equivalent, observed historic values (+), linear least squares regression (green) and orthogonal least squares regression (red); upper right panel, same as upper left panel but for base flow; lower left panel, same as upper left panel but for peak flow timing; and lower right panel, same as upper left panel but for base flow timing.

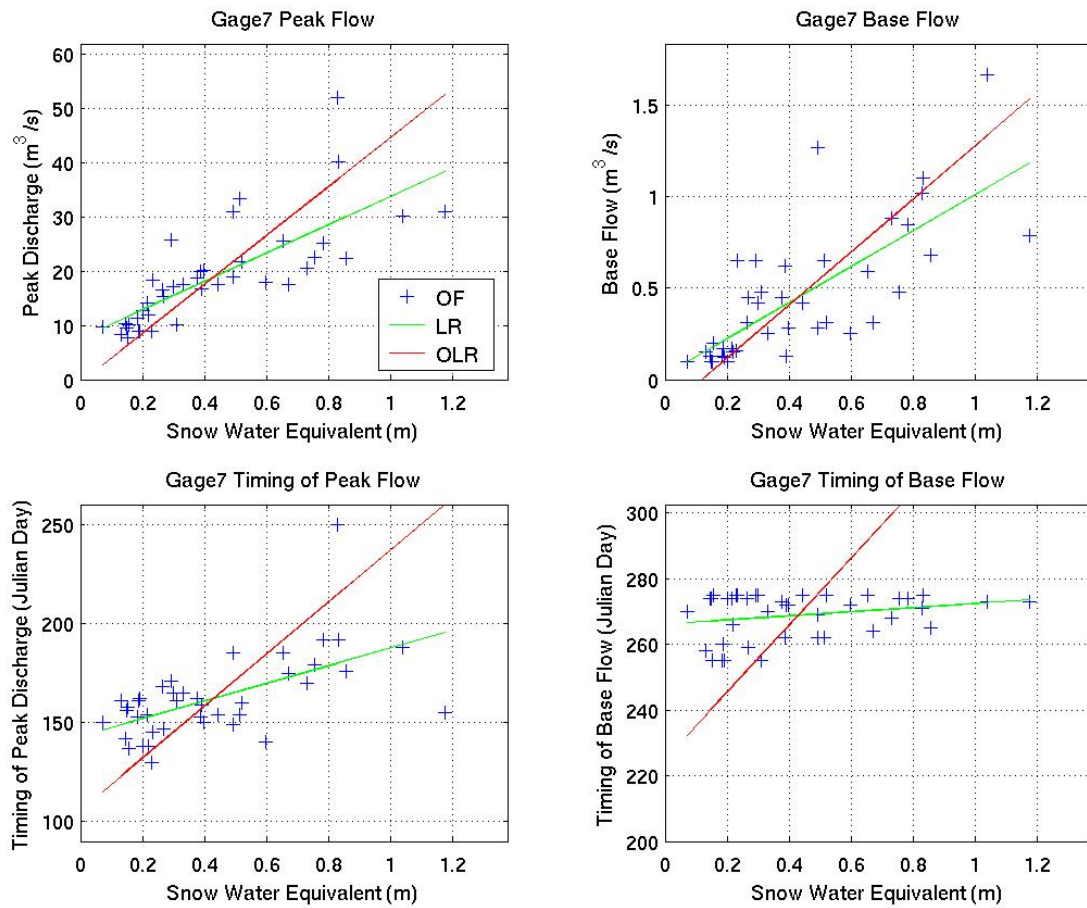


Fig. D7. Bear Creek Upper left panel, peak flow as a linear function of snow water equivalent, observed historic values (+), linear least squares regression (green) and orthogonal least squares regression (red); upper right panel, same as upper left panel but for base flow; lower left panel, same as upper left panel but for peak flow timing; and lower right panel, same as upper left panel but for base flow timing.

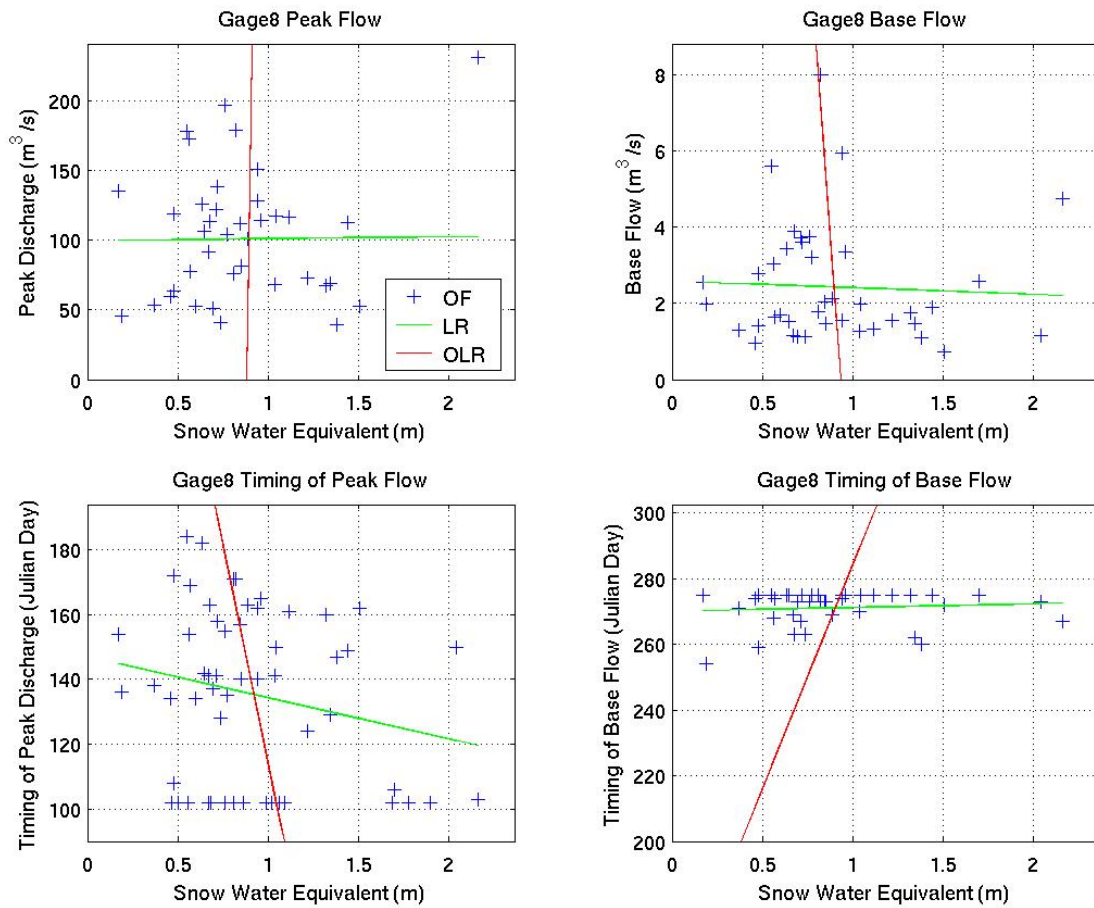


Fig. D8. San Joaquin at Millers Crossing Upper left panel, peak flow as a linear function of snow water equivalent, observed historic values (+), linear least squares regression (green) and orthogonal least squares regression (red); upper right panel, same as upper left panel but for base flow; lower left panel, same as upper left panel but for peak flow timing; and lower right panel, same as upper left panel but for base flow timing.

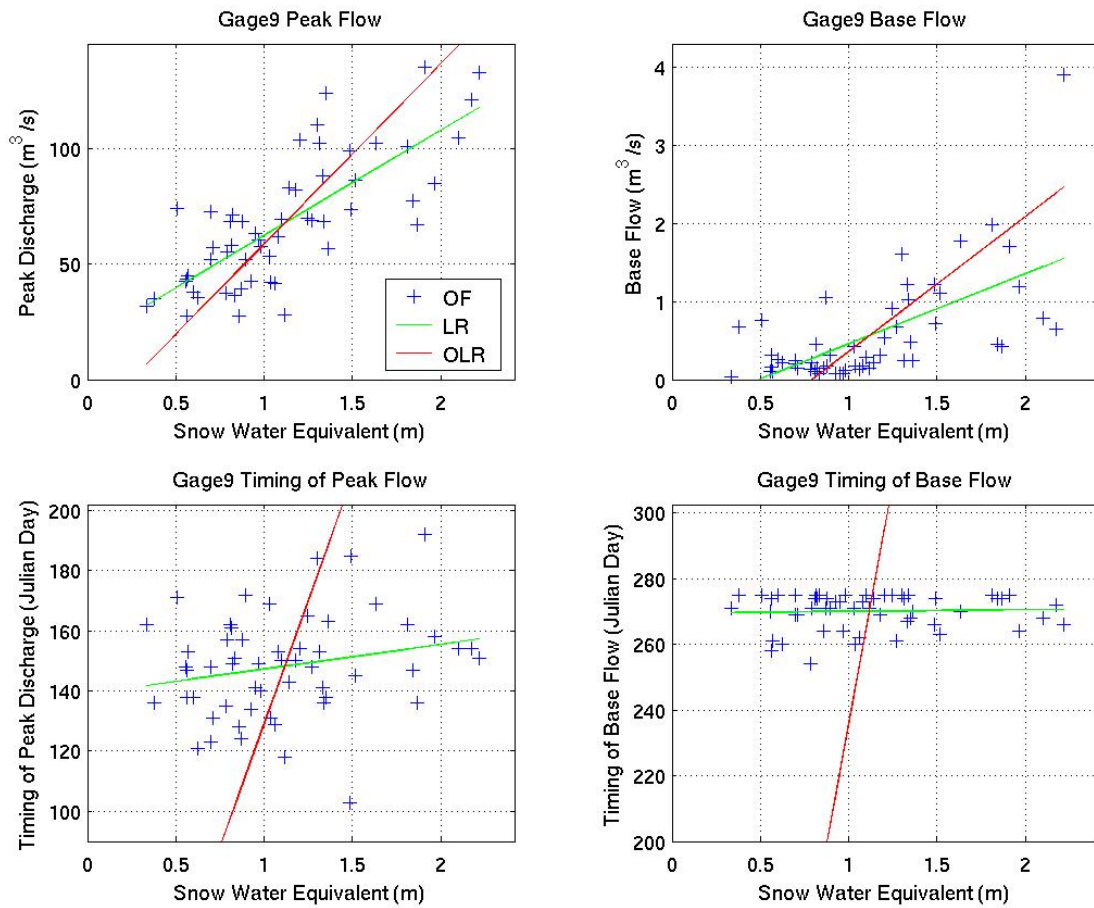


Fig. D9. Merced at Happy Isles Upper left panel, peak flow as a linear function of snow water equivalent, observed historic values (+), linear least squares regression (green) and orthogonal least squares regression (red); upper right panel, same as upper left panel but for base flow; lower left panel, same as upper left panel but for peak flow timing; and lower right panel, same as upper left panel but for base flow timing.

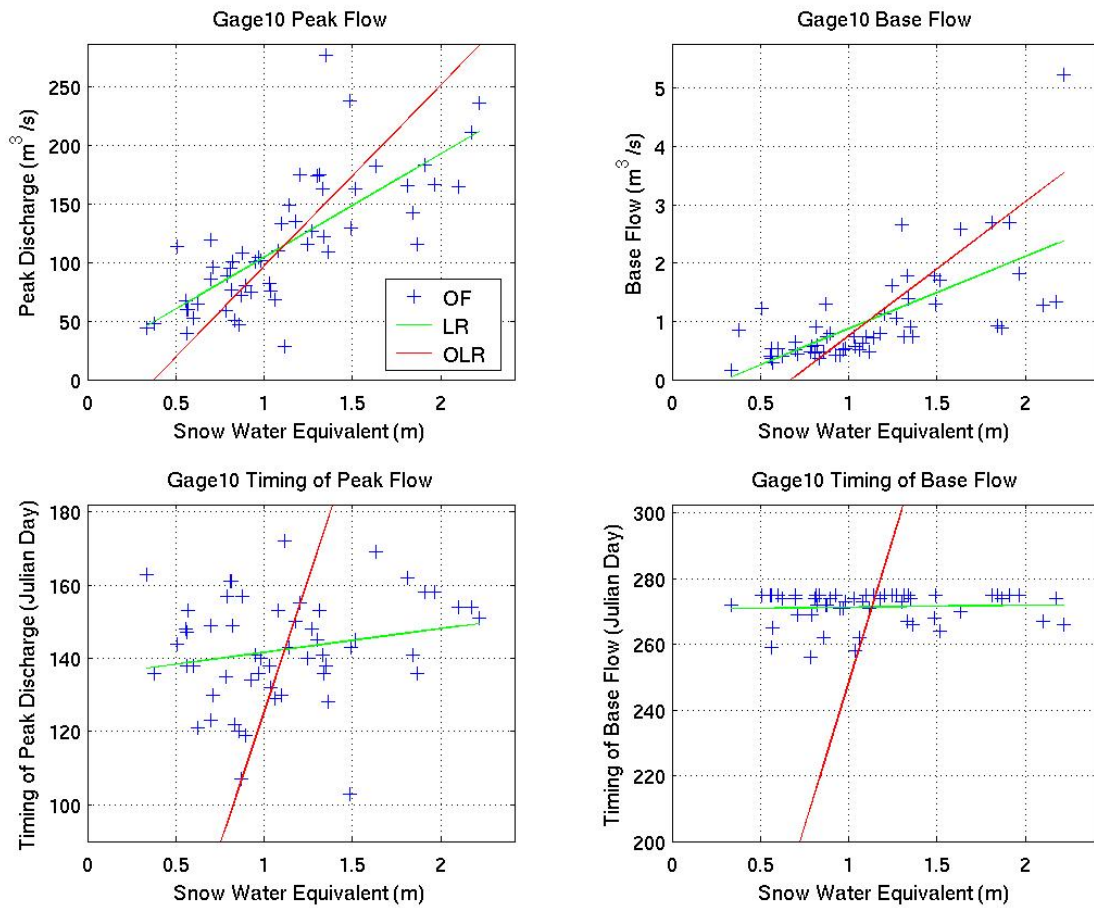


Fig. D10. Merced at Pohono Upper left panel, peak flow as a linear function of snow water equivalent, observed historic values (+), linear least squares regression (green) and orthogonal least squares regression (red); upper right panel, same as upper left panel but for base flow; lower left panel, same as upper left panel but for peak flow timing; and lower right panel, same as upper left panel but for base flow timing.

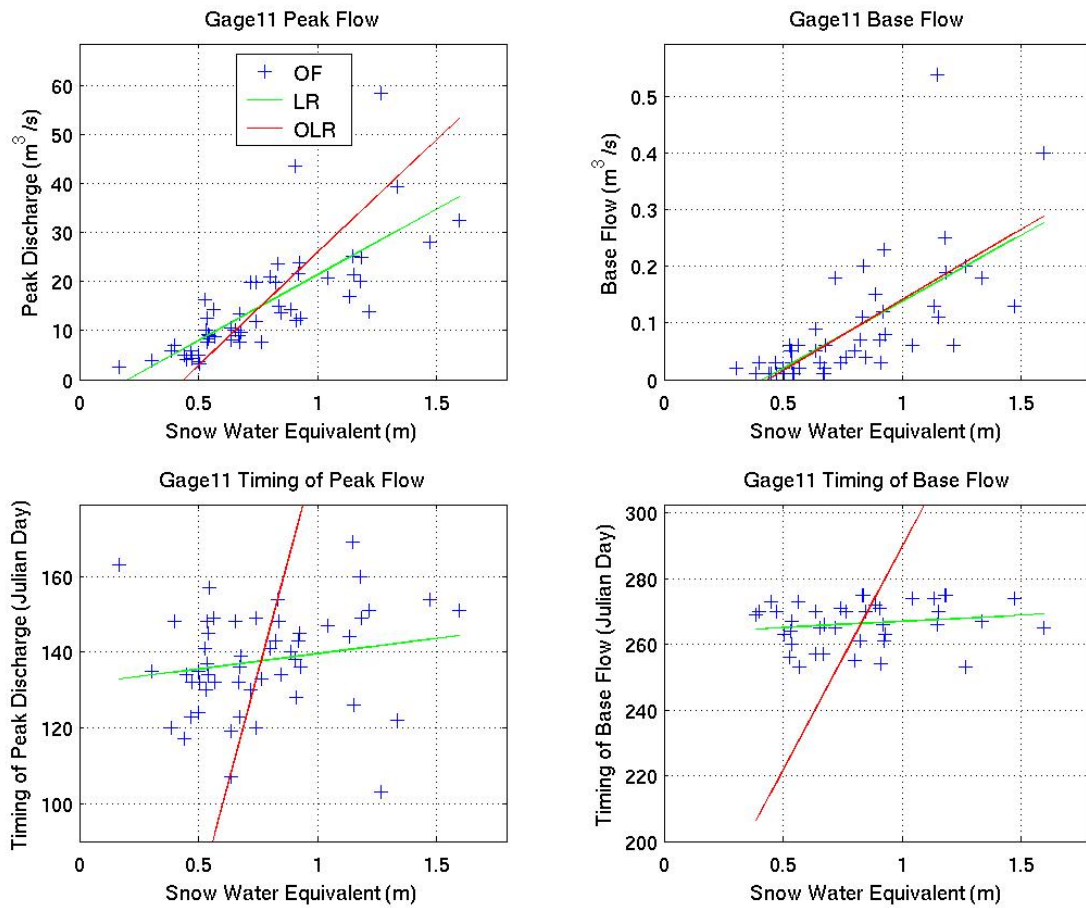


Fig. D11. Middle Fork Tuolumne Upper left panel, peak flow as a linear function of snow water equivalent, observed historic values (+), linear least squares regression (green) and orthogonal least squares regression (red); upper right panel, same as upper left panel but for base flow; lower left panel, same as upper left panel but for peak flow timing; and lower right panel, same as upper left panel but for base flow timing.

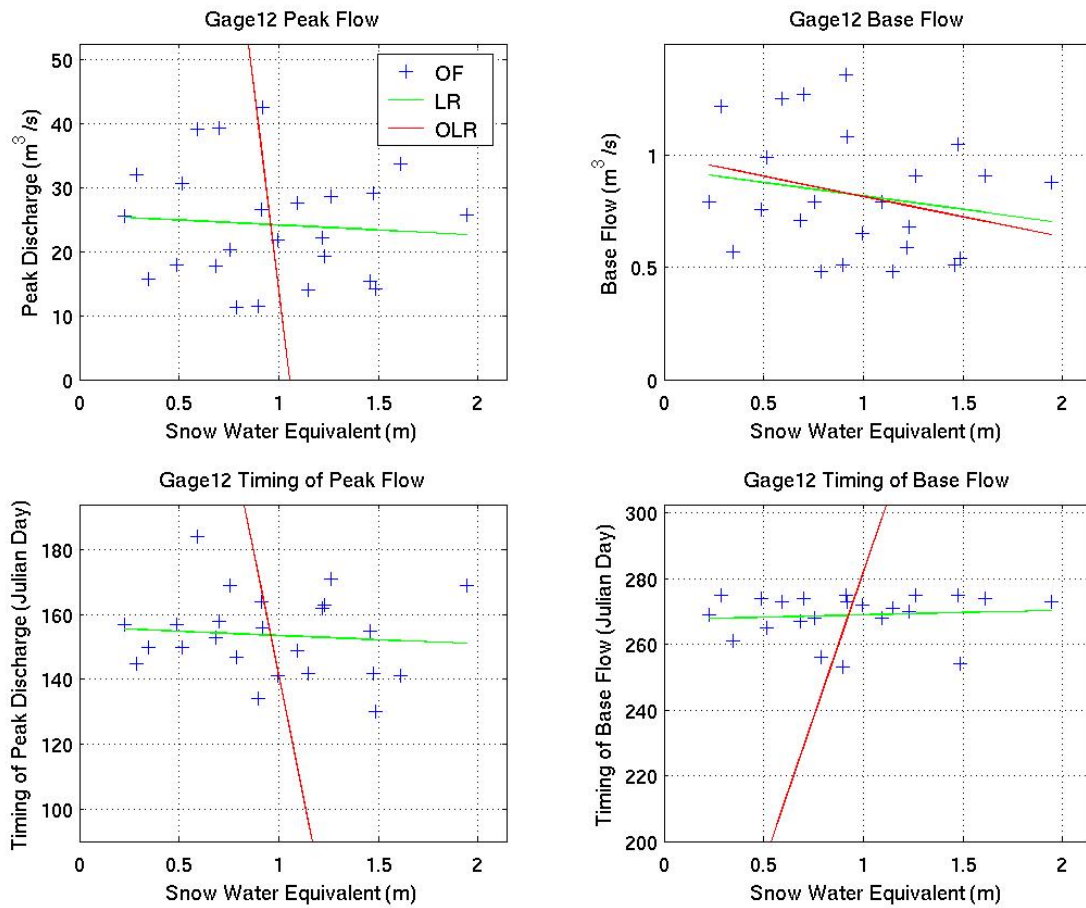


Fig. D12. Stanislaus at Clark Fork Upper left panel, peak flow as a linear function of snow water equivalent, observed historic values (+), linear least squares regression (green) and orthogonal least squares regression (red); upper right panel, same as upper left panel but for base flow; lower left panel, same as upper left panel but for peak flow timing; and lower right panel, same as upper left panel but for base flow timing.

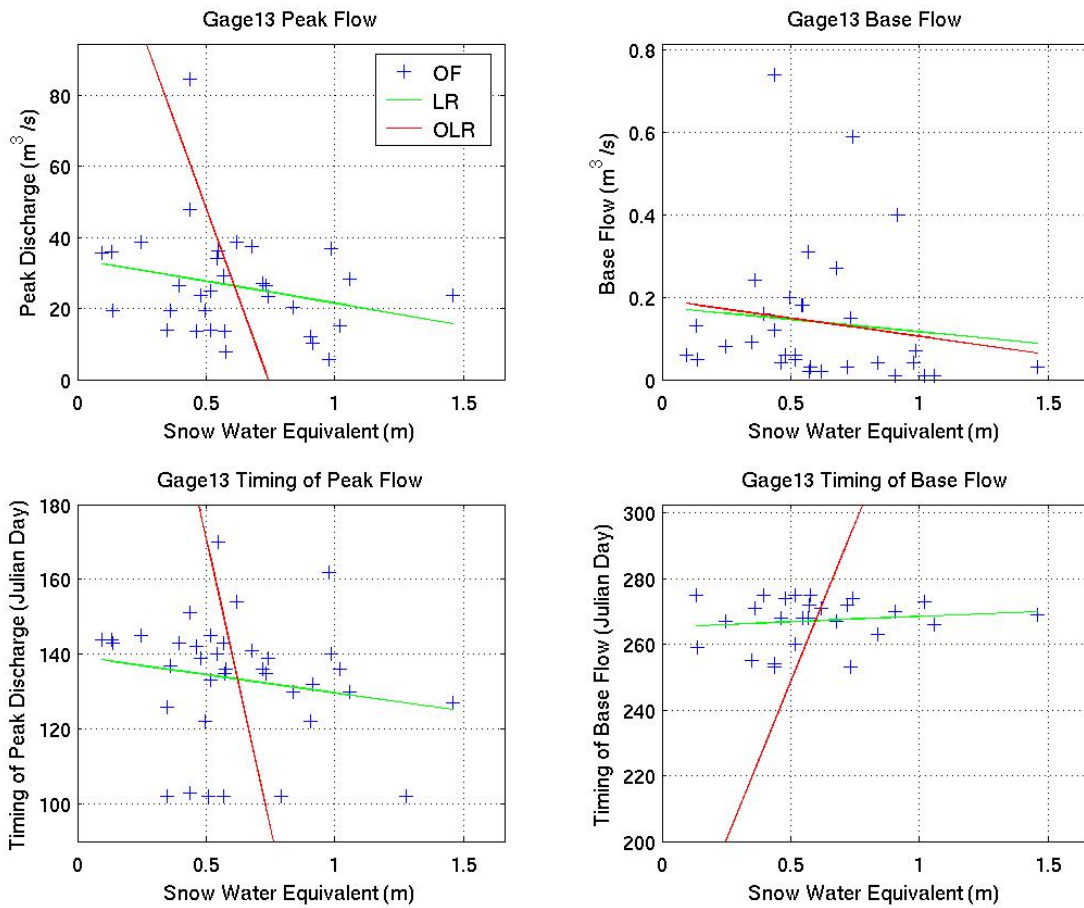


Fig. D13. Highland Creek Upper left panel, peak flow as a linear function of snow water equivalent, observed historic values (+), linear least squares regression (green) and orthogonal least squares regression (red); upper right panel, same as upper left panel but for base flow; lower left panel, same as upper left panel but for peak flow timing; and lower right panel, same as upper left panel but for base flow timing.

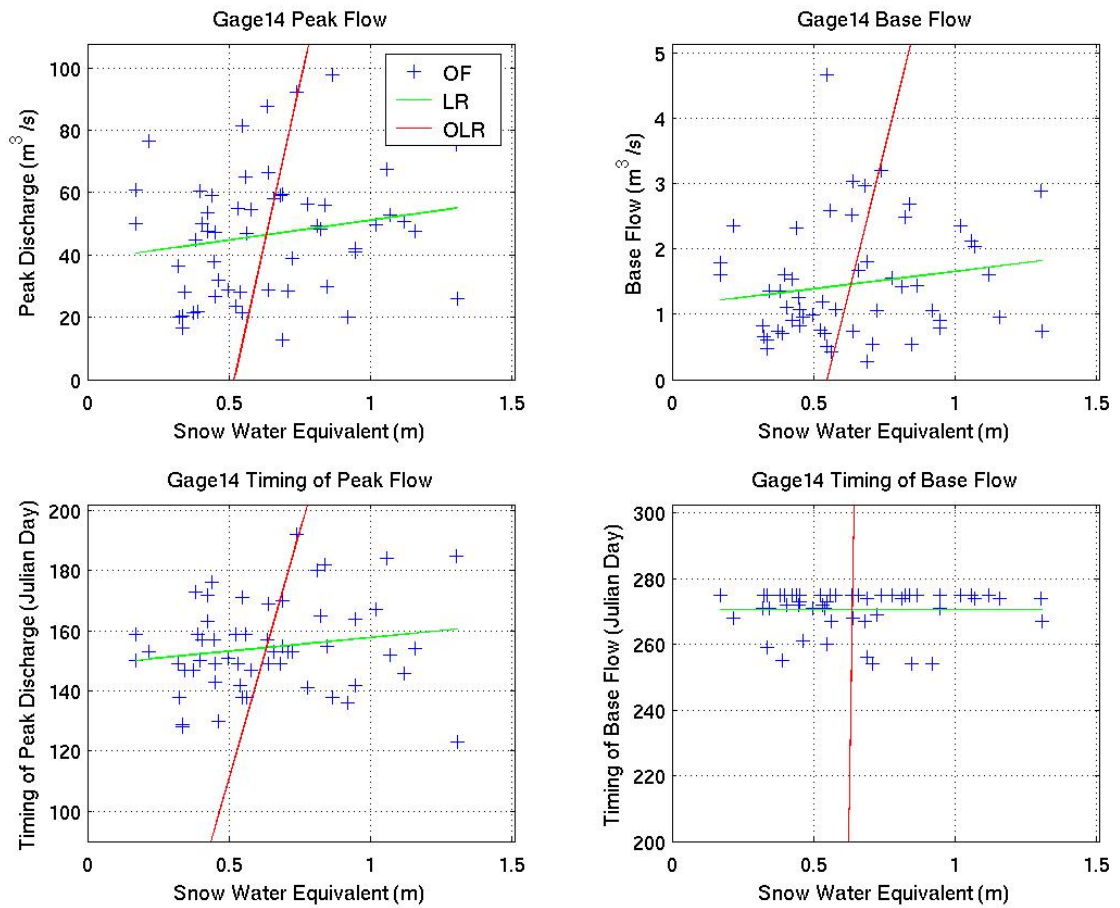


Fig. D14. West Walker Upper left panel, peak flow as a linear function of snow water equivalent, observed historic values (+), linear least squares regression (green) and orthogonal least squares regression (red); upper right panel, same as upper left panel but for base flow; lower left panel, same as upper left panel but for peak flow timing; and lower right panel, same as upper left panel but for base flow timing.

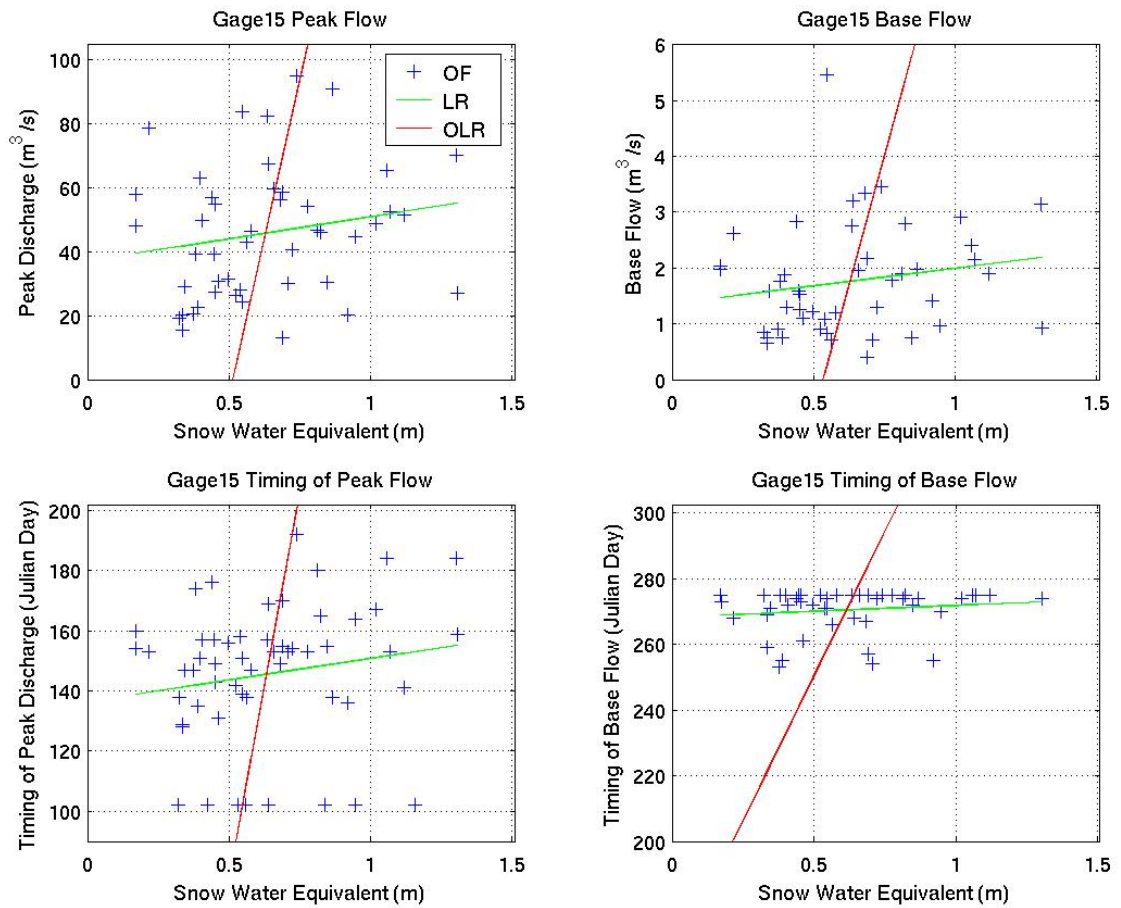


Fig. D15. West Walker near Colville Upper left panel, peak flow as a linear function of snow water equivalent, observed historic values (+), linear least squares regression (green) and orthogonal least squares regression (red); upper right panel, same as upper left panel but for base flow; lower left panel, same as upper left panel but for peak flow timing; and lower right panel, same as upper left panel but for base flow timing.

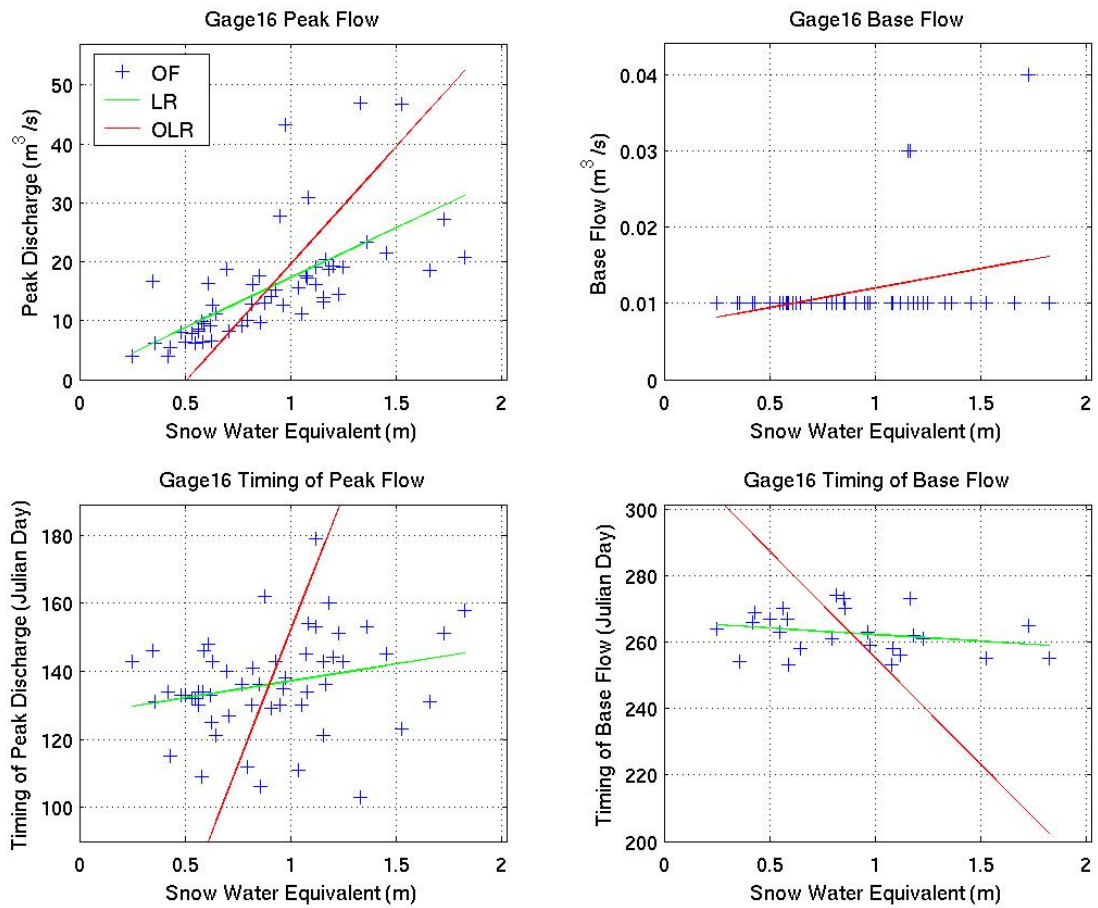


Fig. D16. Cole Creek Upper left panel, peak flow as a linear function of snow water equivalent, observed historic values (+), linear least squares regression (green) and orthogonal least squares regression (red); upper right panel, same as upper left panel but for base flow; lower left panel, same as upper left panel but for peak flow timing; and lower right panel, same as upper left panel but for base flow timing.

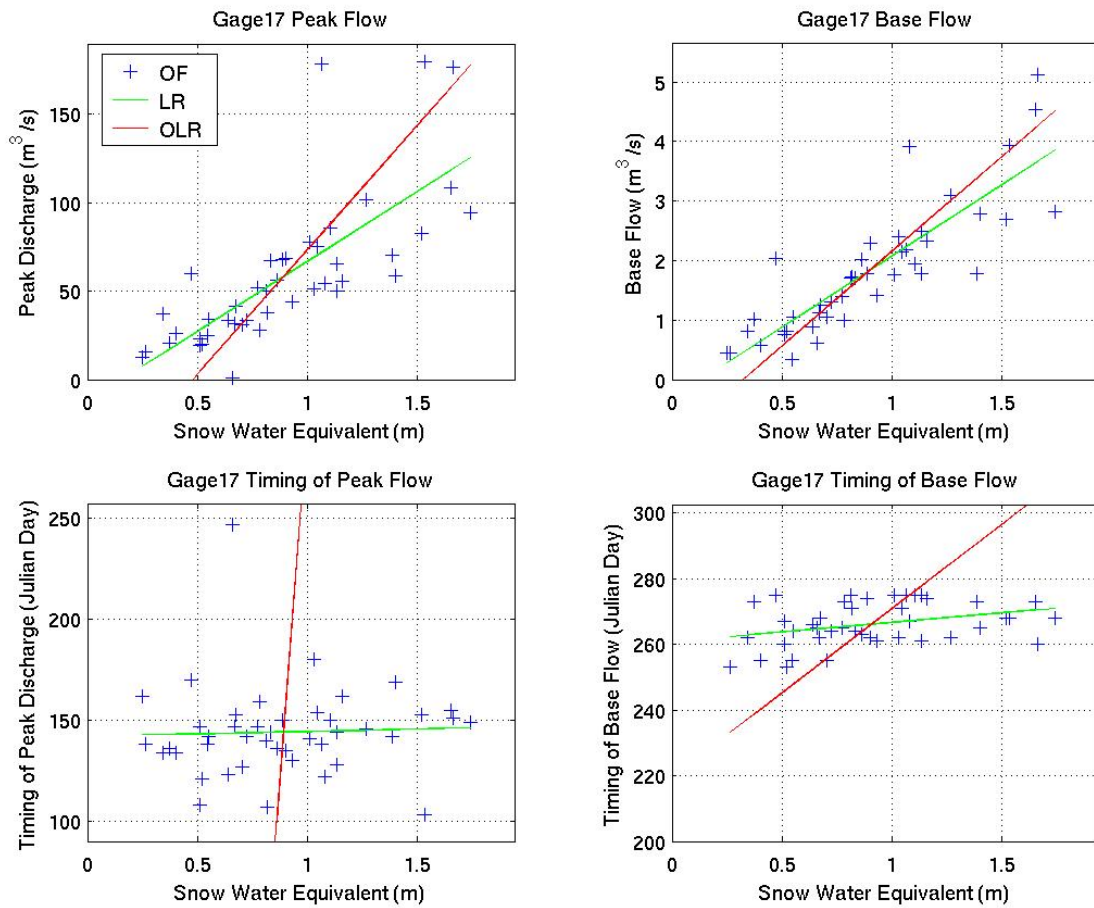


Fig. D17. East Fork Carson Upper left panel, peak flow as a linear function of snow water equivalent, observed historic values (+), linear least squares regression (green) and orthogonal least squares regression (red); upper right panel, same as upper left panel but for base flow; lower left panel, same as upper left panel but for peak flow timing; and lower right panel, same as upper left panel but for base flow timing.

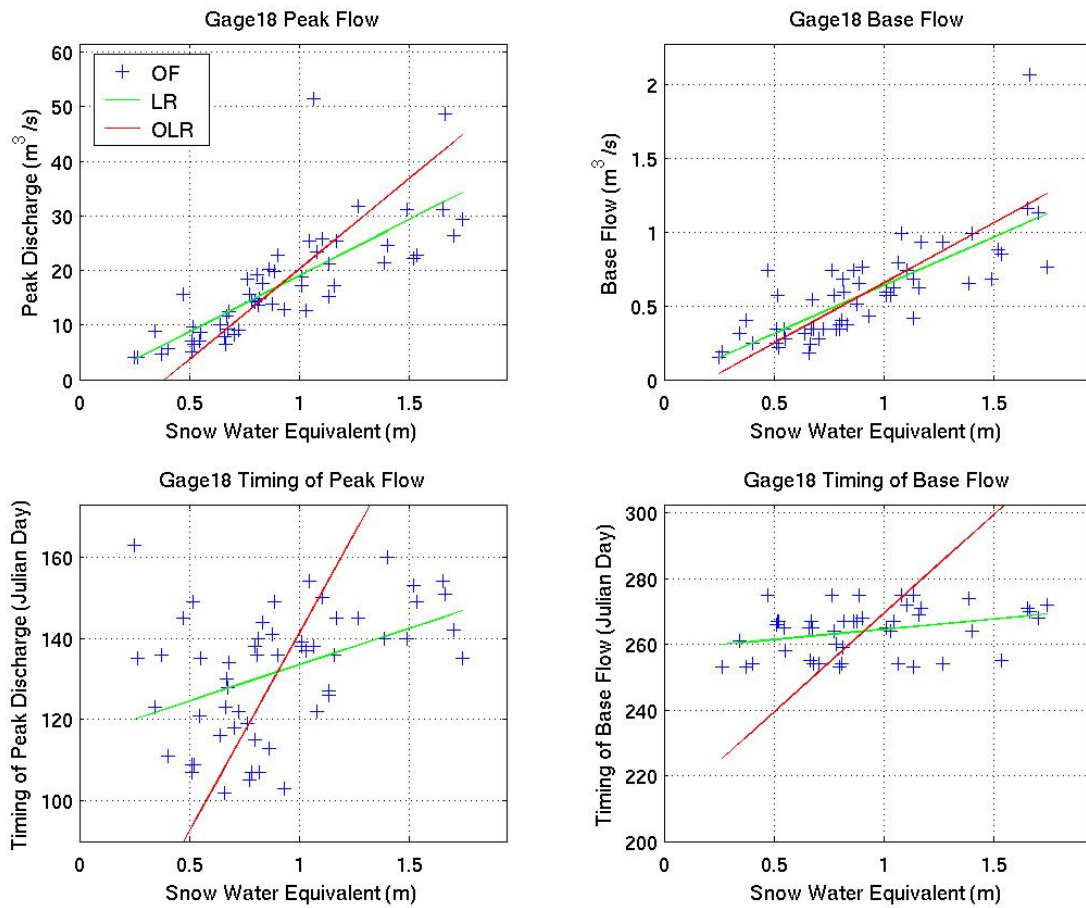


Fig. D18. West Fork Carson Upper left panel, peak flow as a linear function of snow water equivalent, observed historic values (+), linear least squares regression (green) and orthogonal least squares regression (red); upper right panel, same as upper left panel but for base flow; lower left panel, same as upper left panel but for peak flow timing; and lower right panel, same as upper left panel but for base flow timing.

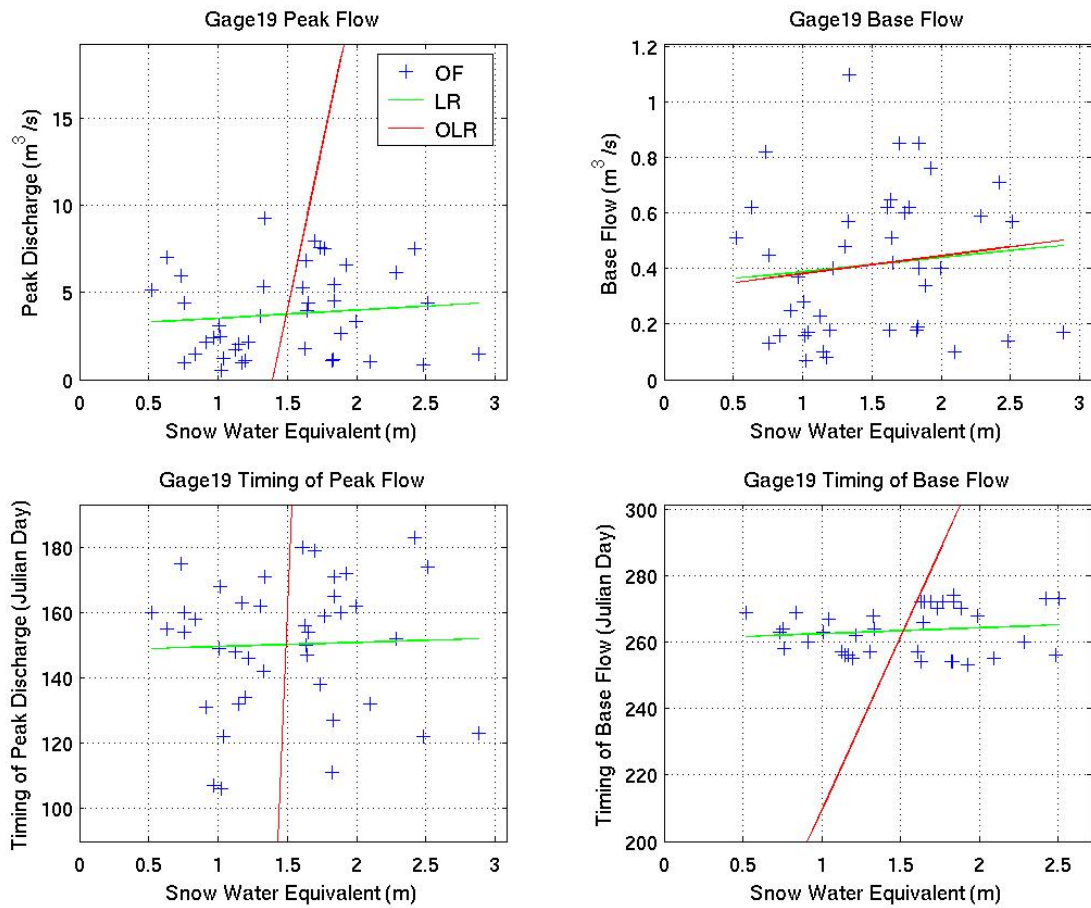


Fig. D19. Trout Creek Upper left panel, peak flow as a linear function of snow water equivalent, observed historic values (+), linear least squares regression (green) and orthogonal least squares regression (red); upper right panel, same as upper left panel but for base flow; lower left panel, same as upper left panel but for peak flow timing; and lower right panel, same as upper left panel but for base flow timing.

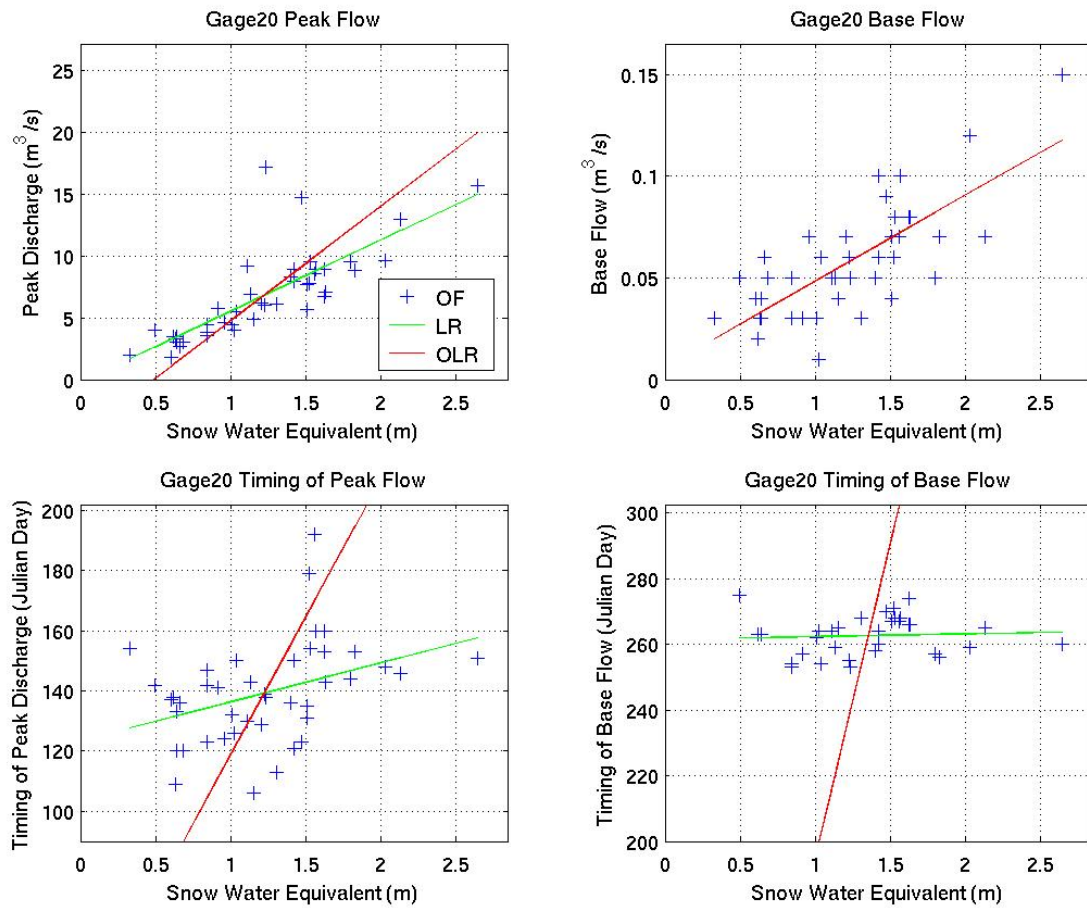


Fig. D20. Blackwood Creek Upper left panel, peak flow as a linear function of snow water equivalent, observed historic values (+), linear least squares regression (green) and orthogonal least squares regression (red); upper right panel, same as upper left panel but for base flow; lower left panel, same as upper left panel but for peak flow timing; and lower right panel, same as upper left panel but for base flow timing.

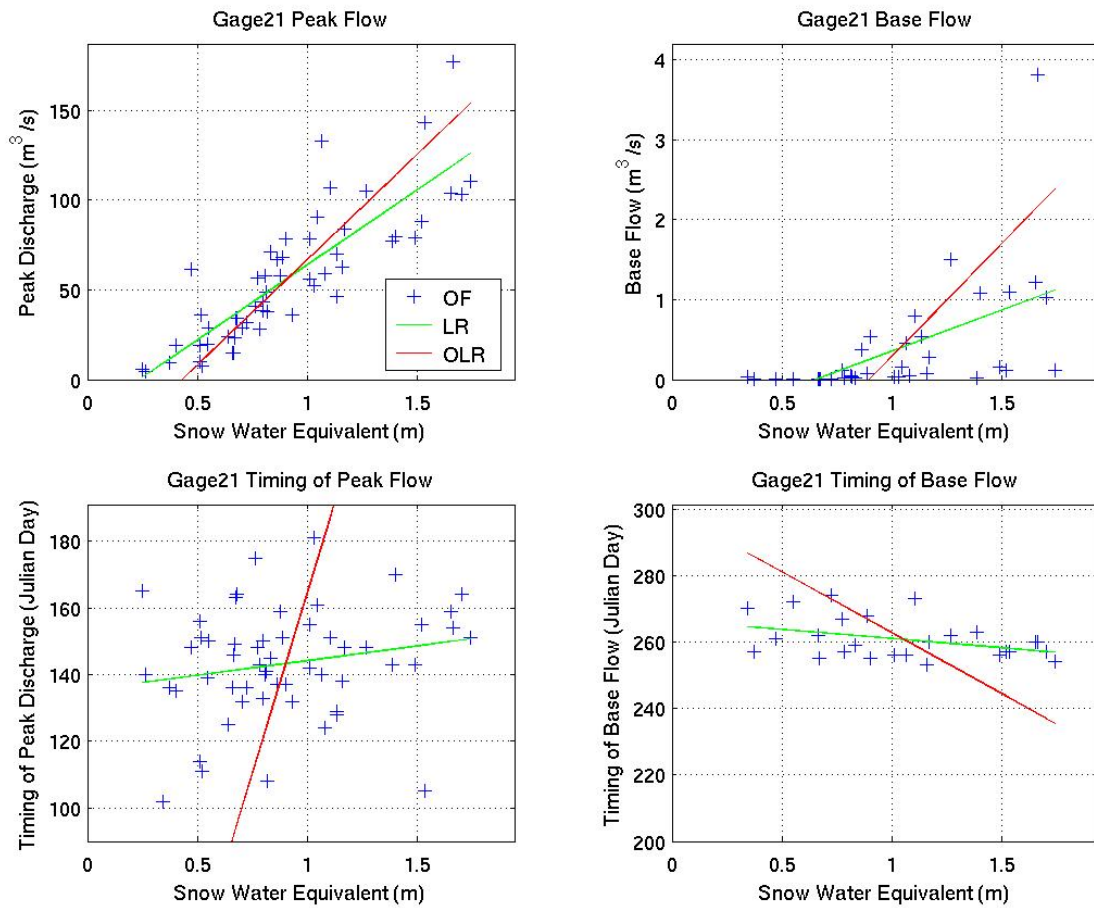


Fig. D21. Carson near Fort Churchill Upper left panel, peak flow as a linear function of snow water equivalent, observed historic values (+), linear least squares regression (green) and orthogonal least squares regression (red); upper right panel, same as upper left panel but for base flow; lower left panel, same as upper left panel but for peak flow timing; and lower right panel, same as upper left panel but for base flow timing.

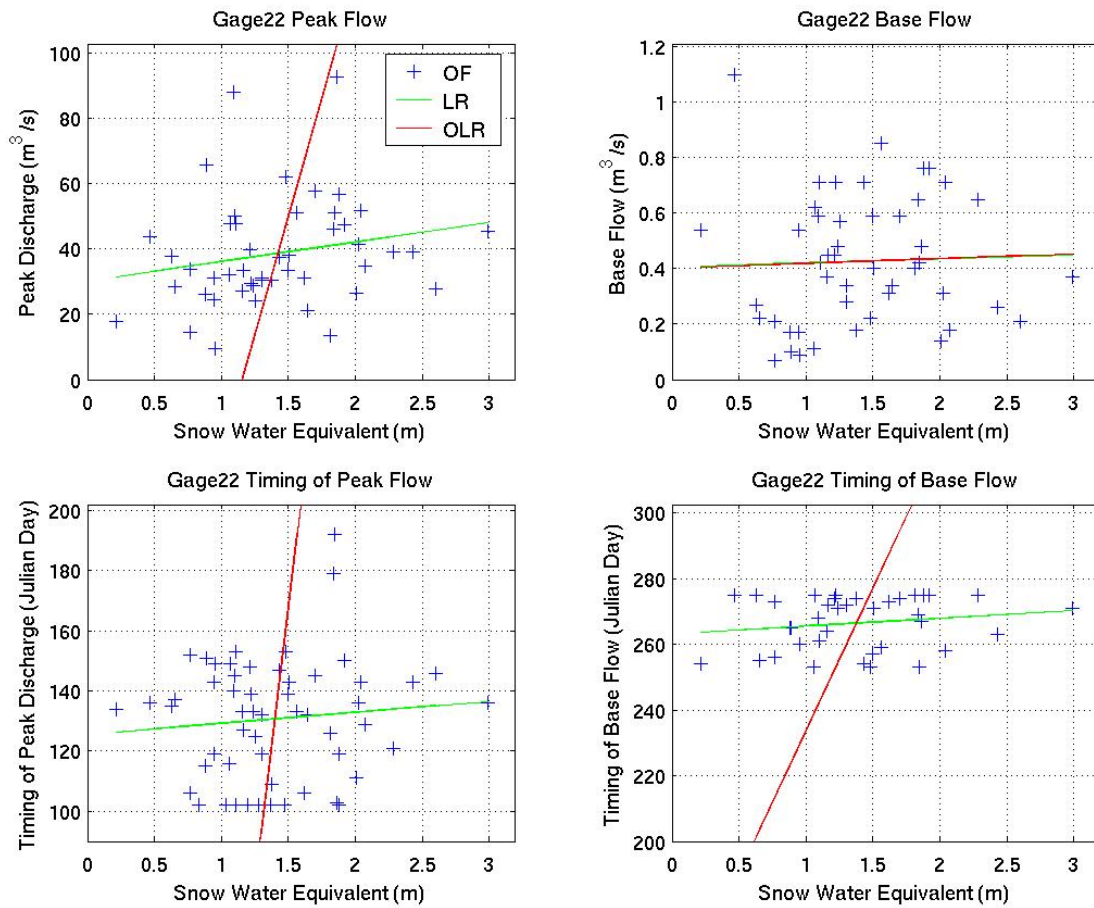


Fig. D22. South Yuba Upper left panel, peak flow as a linear function of snow water equivalent, observed historic values (+), linear least squares regression (green) and orthogonal least squares regression (red); upper right panel, same as upper left panel but for base flow; lower left panel, same as upper left panel but for peak flow timing; and lower right panel, same as upper left panel but for base flow timing.

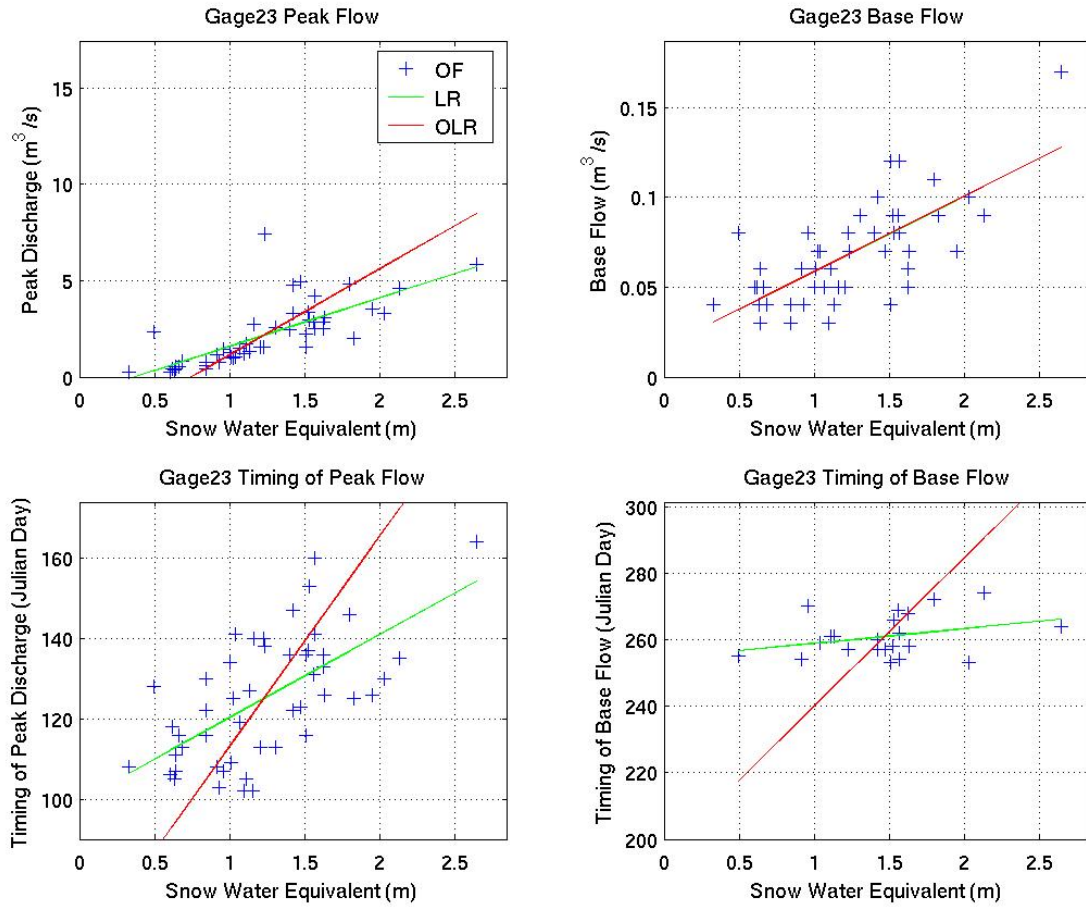


Fig. D23. Sagehen Creek Upper left panel, peak flow as a linear function of snow water equivalent, observed historic values (+), linear least squares regression (green) and orthogonal least squares regression (red); upper right panel, same as upper left panel but for base flow; lower left panel, same as upper left panel but for peak flow timing; and lower right panel, same as upper left panel but for base flow timing.

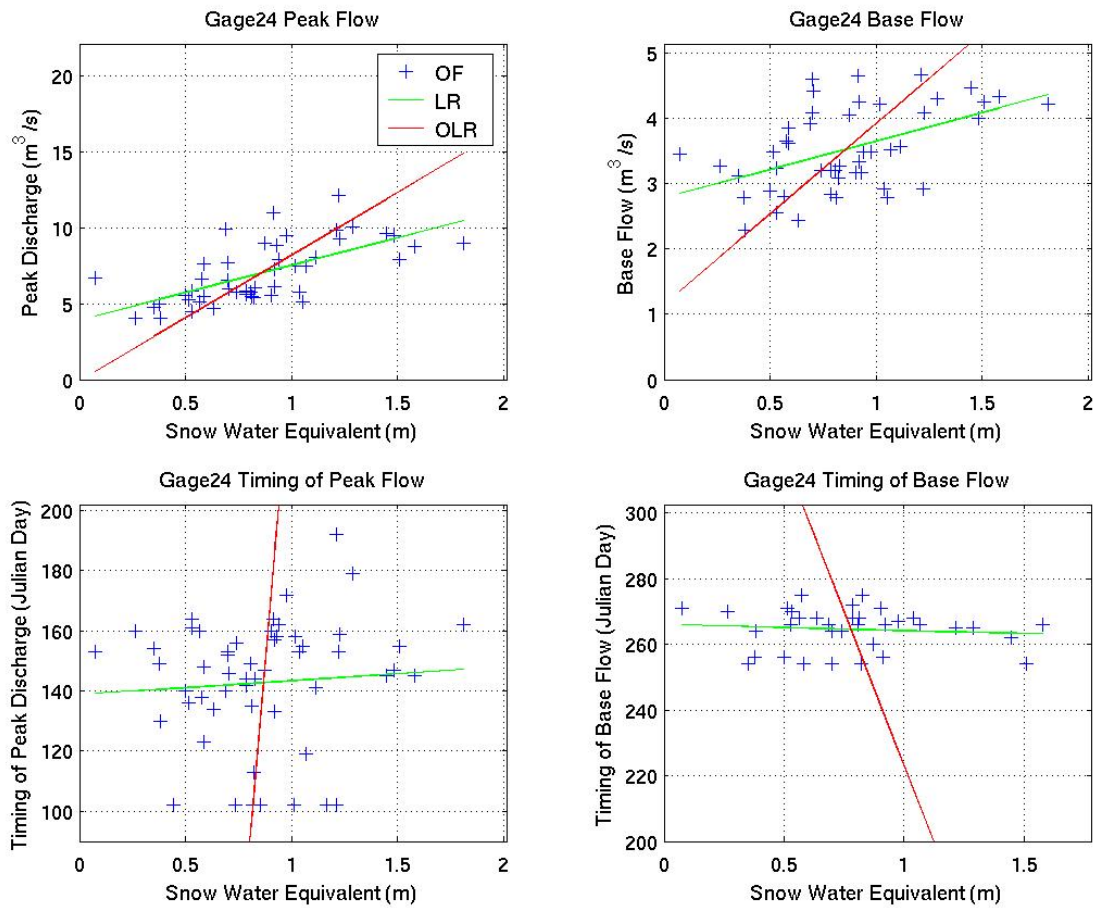


Fig. D24. Hat Creek Upper left panel, peak flow as a linear function of snow water equivalent, observed historic values (+), linear least squares regression (green) and orthogonal least squares regression (red); upper right panel, same as upper left panel but for base flow; lower left panel, same as upper left panel but for peak flow timing; and lower right panel, same as upper left panel but for base flow timing.

APPENDIX E INTRABASIN PEAK/BASE CORRELATIONS

South to north plots of peak and base flow with respect to time in the upper panel and base flow with respect to peak flow in the lower panel.

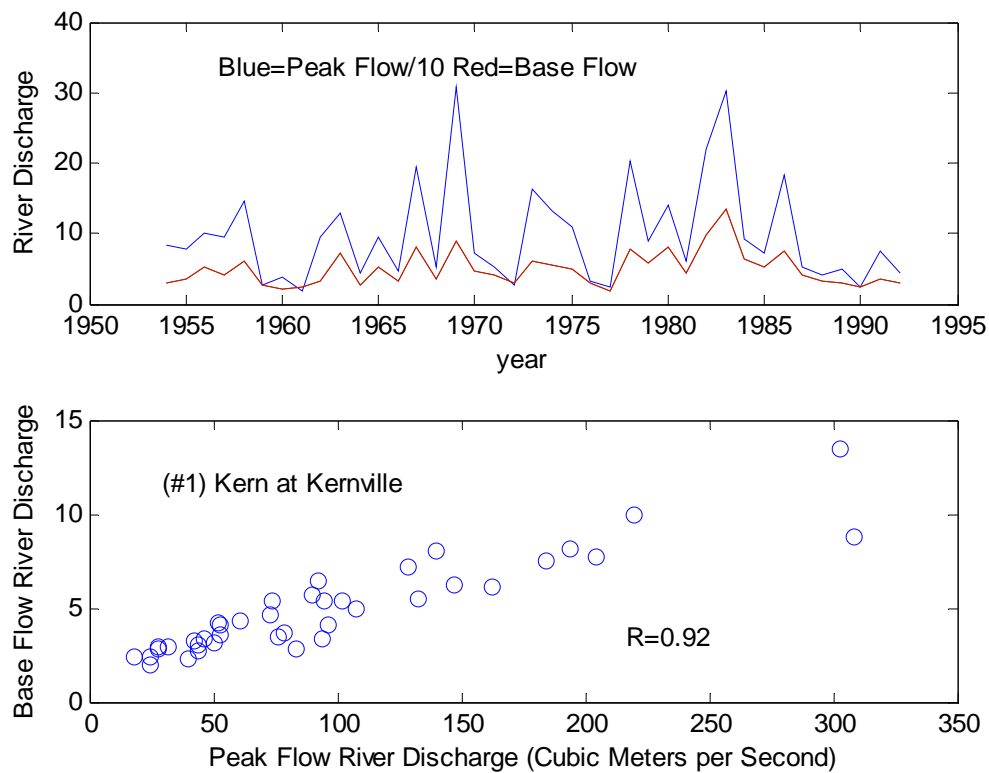


Fig. E1. Upper Panel, time series of peak flow divided by 10 (blue) and base flow (red). Lower Panel, Base flow as a linear function of peak flow. Note base flow in 1983 is higher than 1969 presumably because 1982 was wet and 1968 was dry.

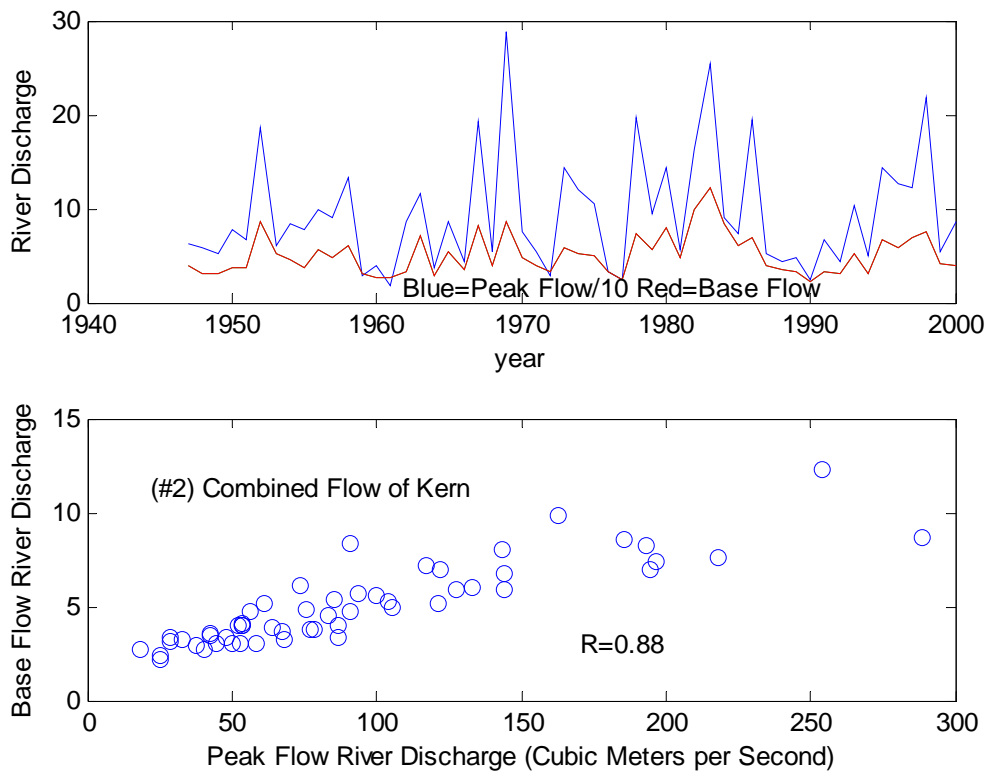


Fig. E2. Upper Panel, time series of peak flow divided by 10 (blue) and base flow (red). Lower Panel, Base flow as a linear function of peak flow.

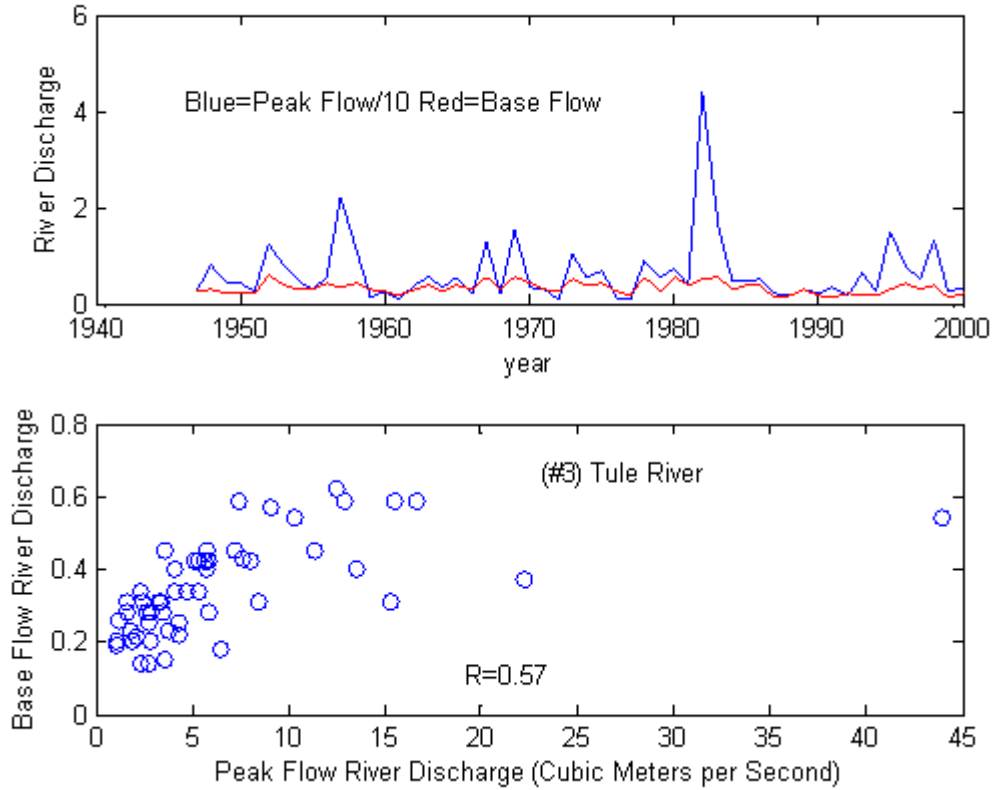


Fig. E3. Upper Panel, time series of peak flow divided by 10 (blue) and base flow (red). Lower Panel, Base flow as a linear function of peak flow. Note, the flat response after $10\text{m}^3\text{ s}^{-1}$ In general, the correlations break down at higher values for reasons not yet fully understood, and more so in some watersheds than others. For example are the flat responses at high flows caused by soil water saturation?

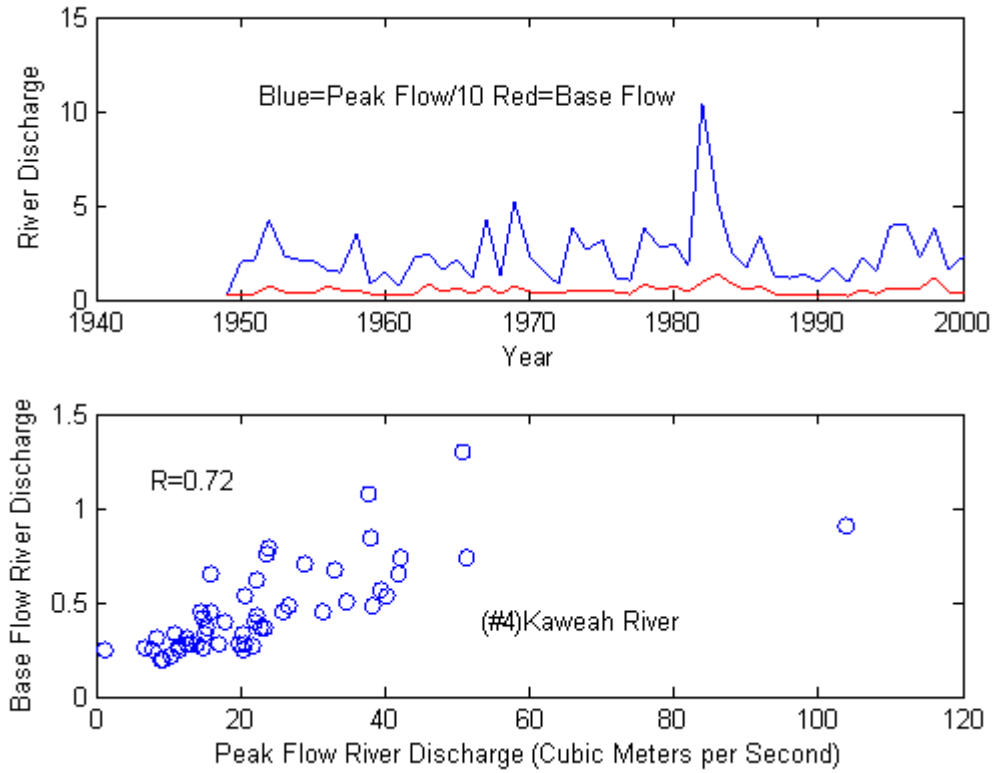


Fig. E4. Upper Panel, time series of peak flow divided by 10 (blue) and base flow (red). Lower Panel, Base flow as a linear function of peak flow.

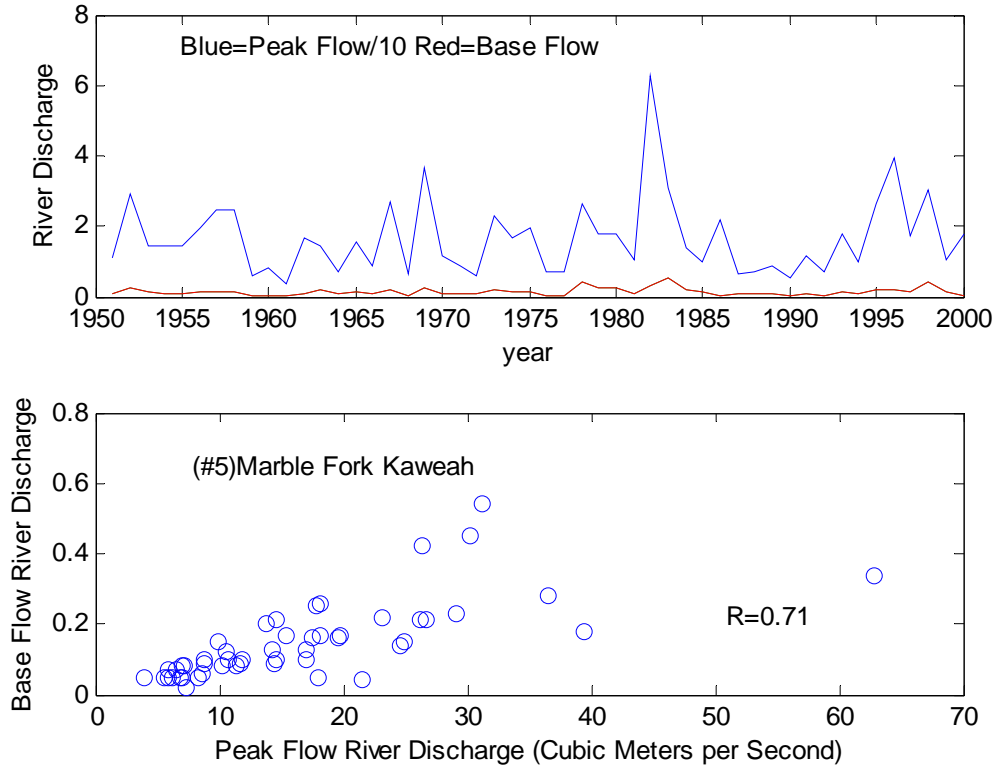


Fig. E5. Upper Panel, time series of peak flow divided by 10 (blue) and base flow (red). Lower Panel, Base flow as a linear function of peak flow.

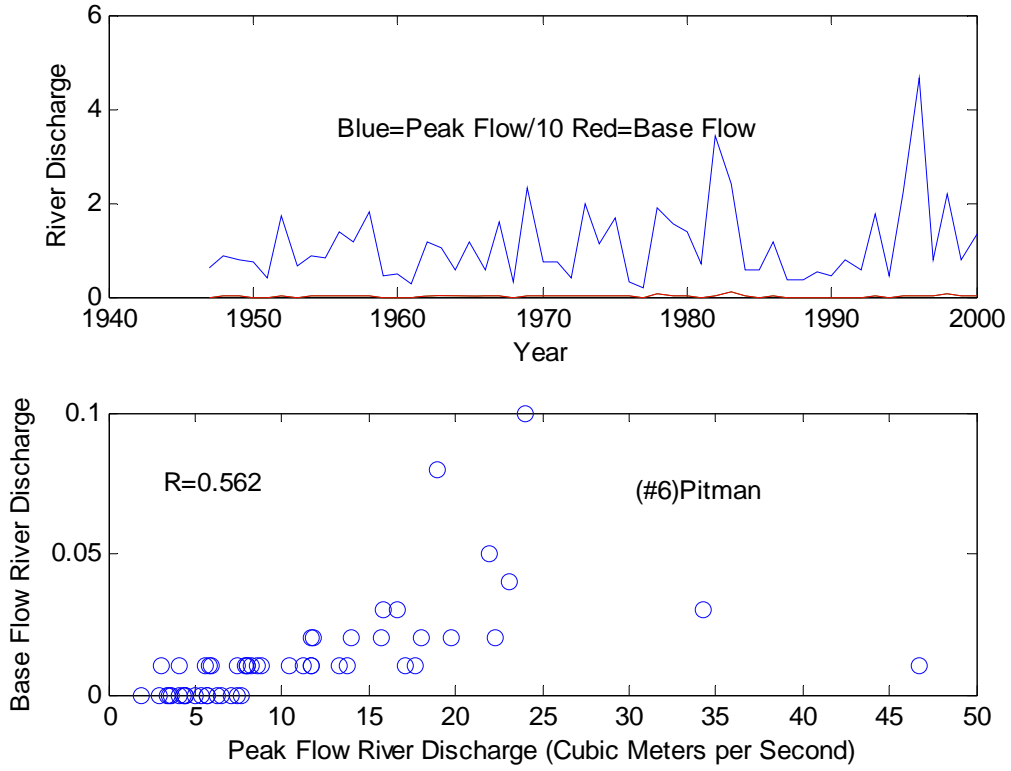


Fig. E6. Upper Panel, time series of peak flow divided by 10 (blue) and base flow (red). Lower Panel, Base flow as a linear function of peak flow.

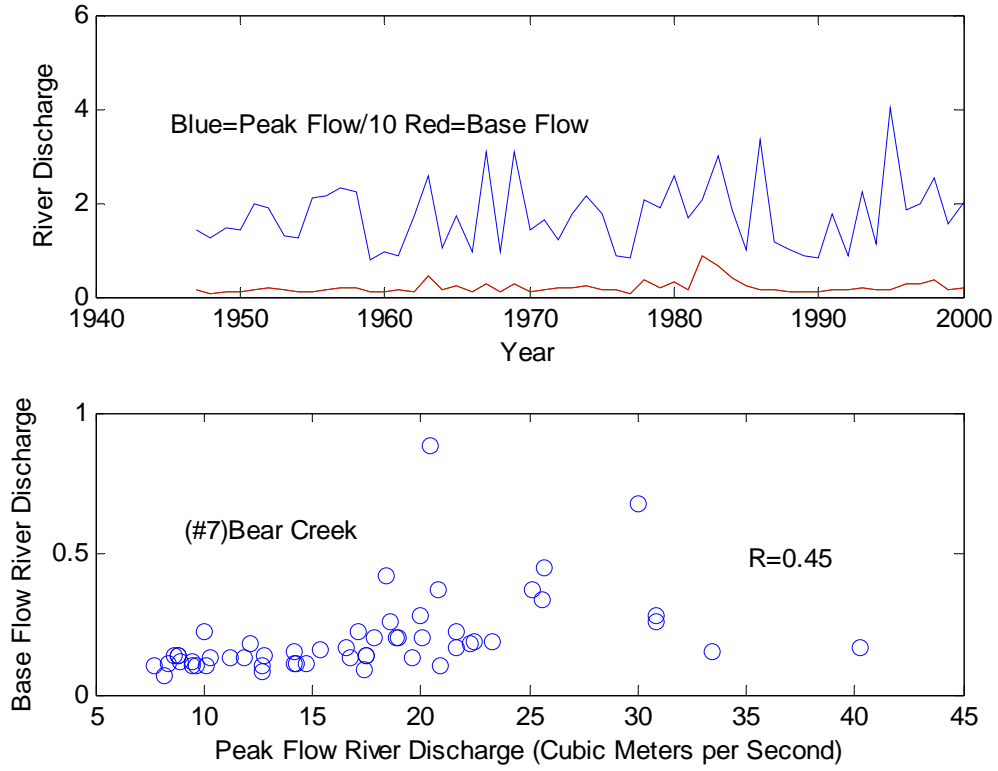


Fig. E7. Upper Panel, time series of peak flow divided by 10 (blue) and base flow (red). Lower Panel, Base flow as a linear function of peak flow.

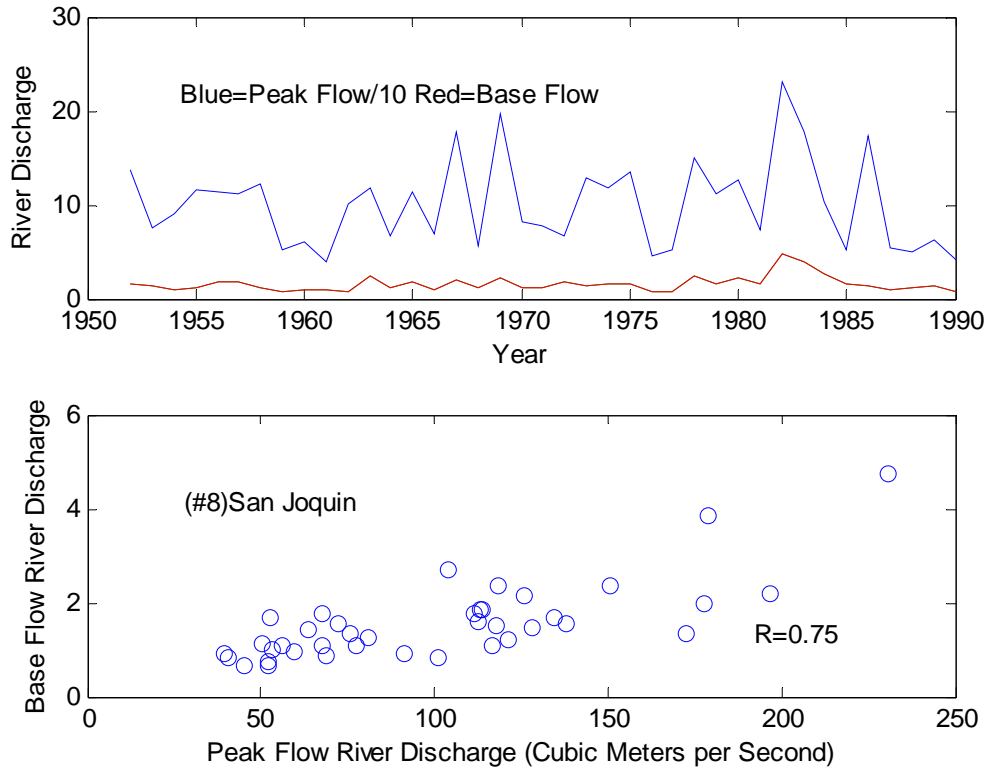


Fig. E8. Upper Panel, time series of peak flow divided by 10 (blue) and base flow (red). Lower Panel, Base flow as a linear function of peak flow.

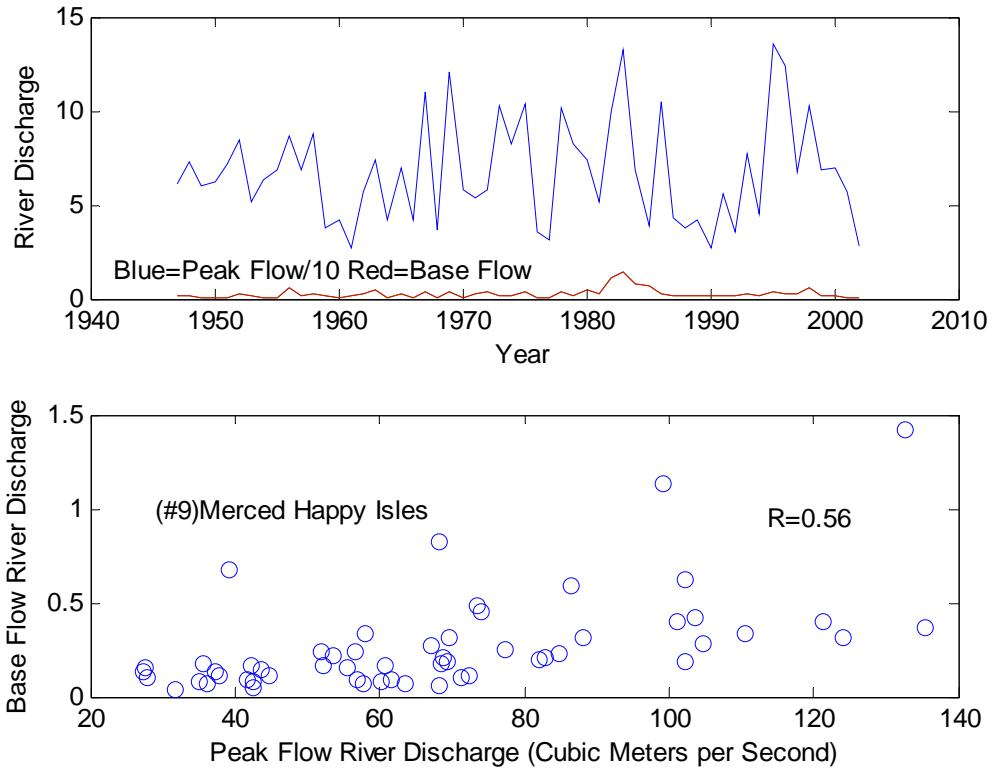


Fig. E9. Upper Panel, time series of peak flow divided by 10 (blue) and base flow (red). Lower Panel, Base flow as a linear function of peak flow.

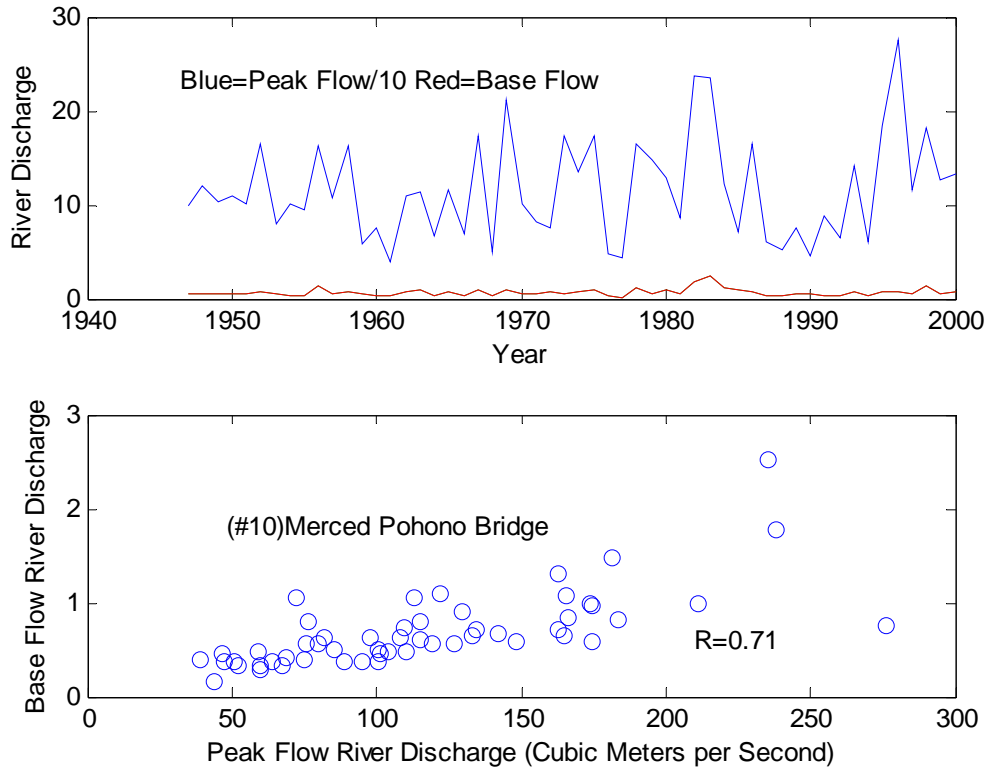


Fig. E10. Upper Panel, time series of peak flow divided by 10 (blue) and base flow (red). Lower Panel, Base flow as a linear function of peak flow.

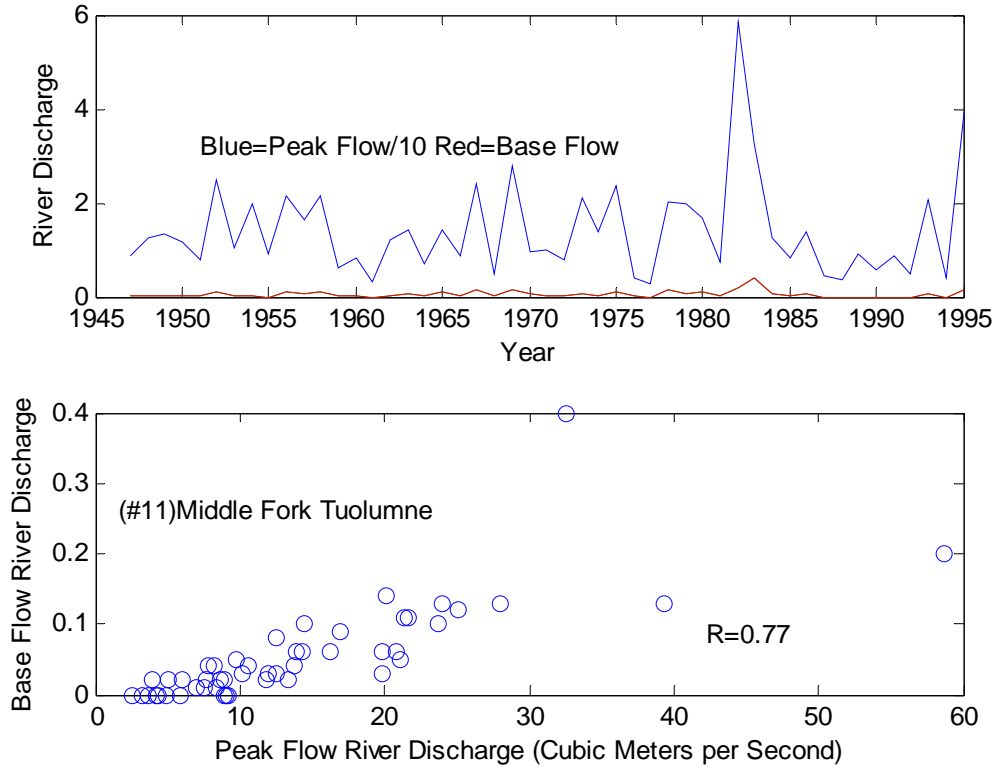


Fig. E11. Upper Panel, time series of peak flow divided by 10 (blue) and base flow (red). Lower Panel, Base flow as a linear function of peak flow.

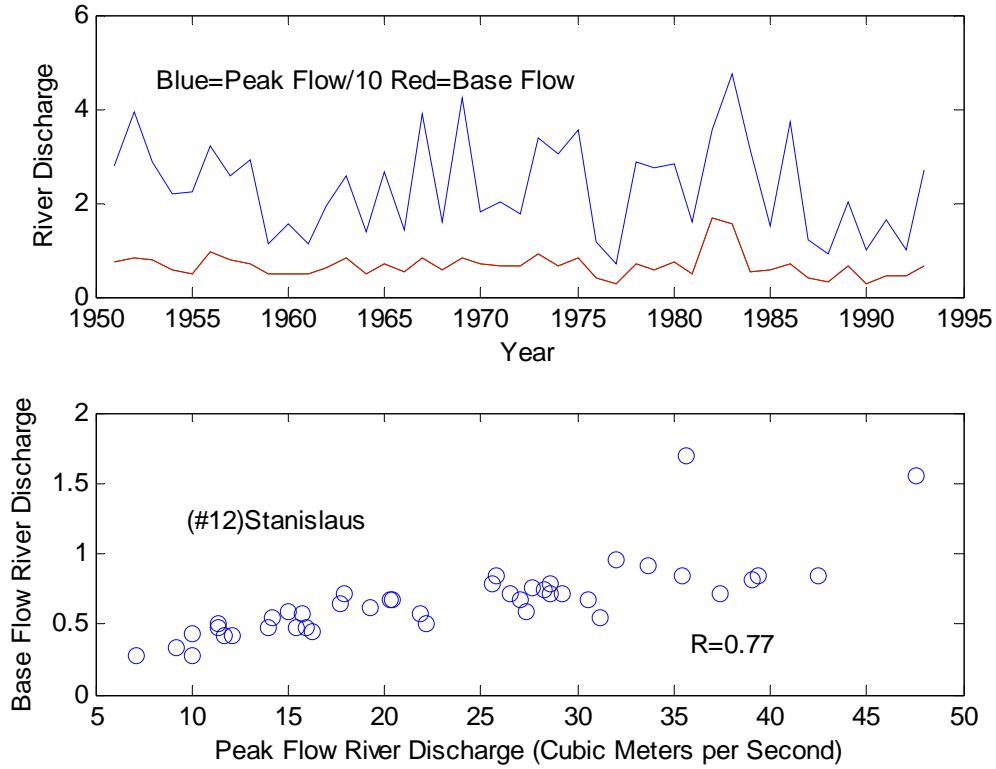


Fig. E12. Upper Panel, time series of peak flow divided by 10 (blue) and base flow (red). Lower Panel, Base flow as a linear function of peak flow.

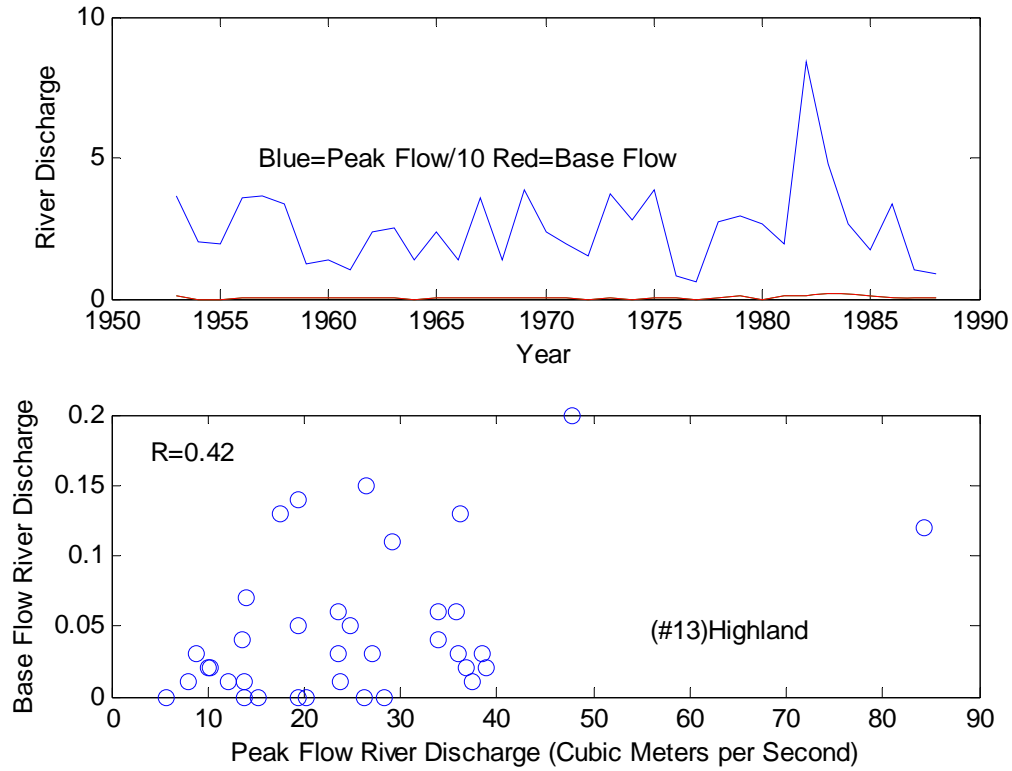


Fig. E13. Upper Panel, time series of peak flow divided by 10 (blue) and base flow (red). Lower Panel, Base flow as a linear function of peak flow.

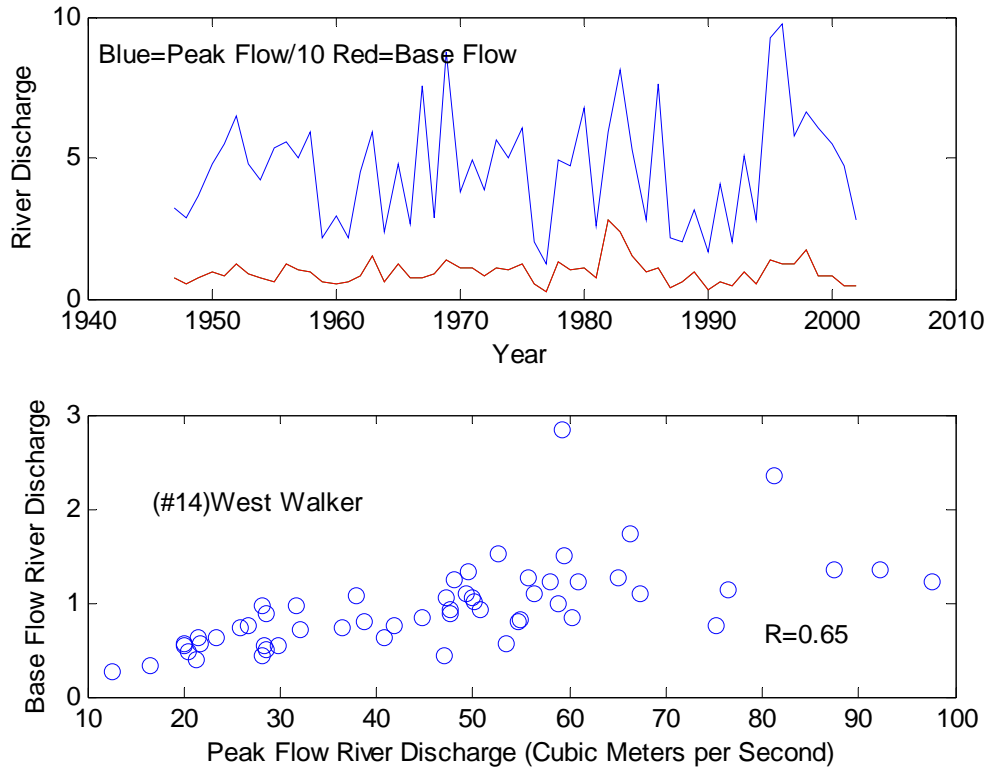


Fig. E14. Upper Panel, time series of peak flow divided by 10 (blue) and base flow (red). Lower Panel, Base flow as a linear function of peak flow.

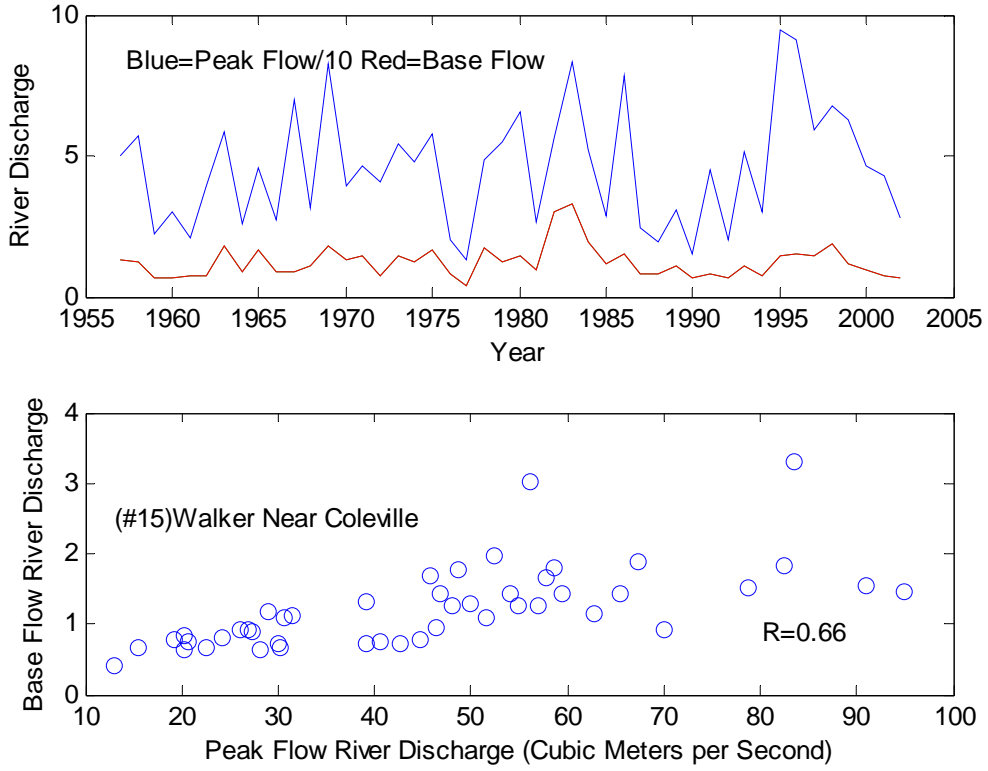


Fig. E15. Upper Panel, time series of peak flow divided by 10 (blue) and base flow (red). Lower Panel, Base flow as a linear function of peak flow.

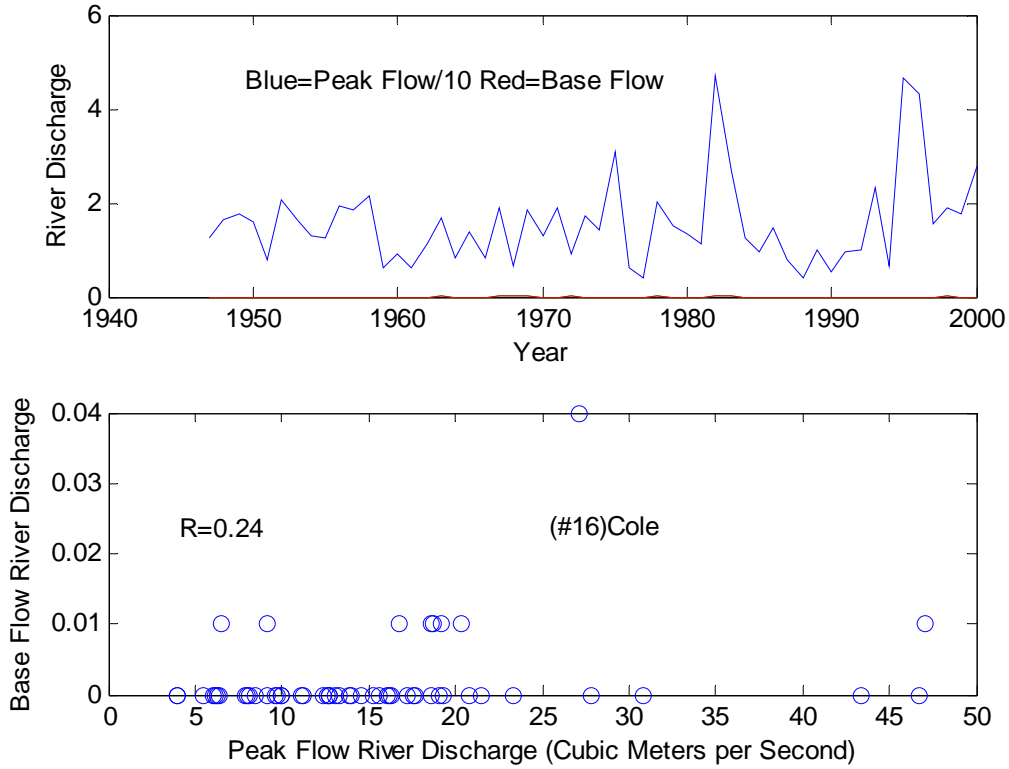


Fig. E16. Upper Panel, time series of peak flow divided by 10 (blue) and base flow (red). Lower Panel, Base flow as a linear function of peak flow.

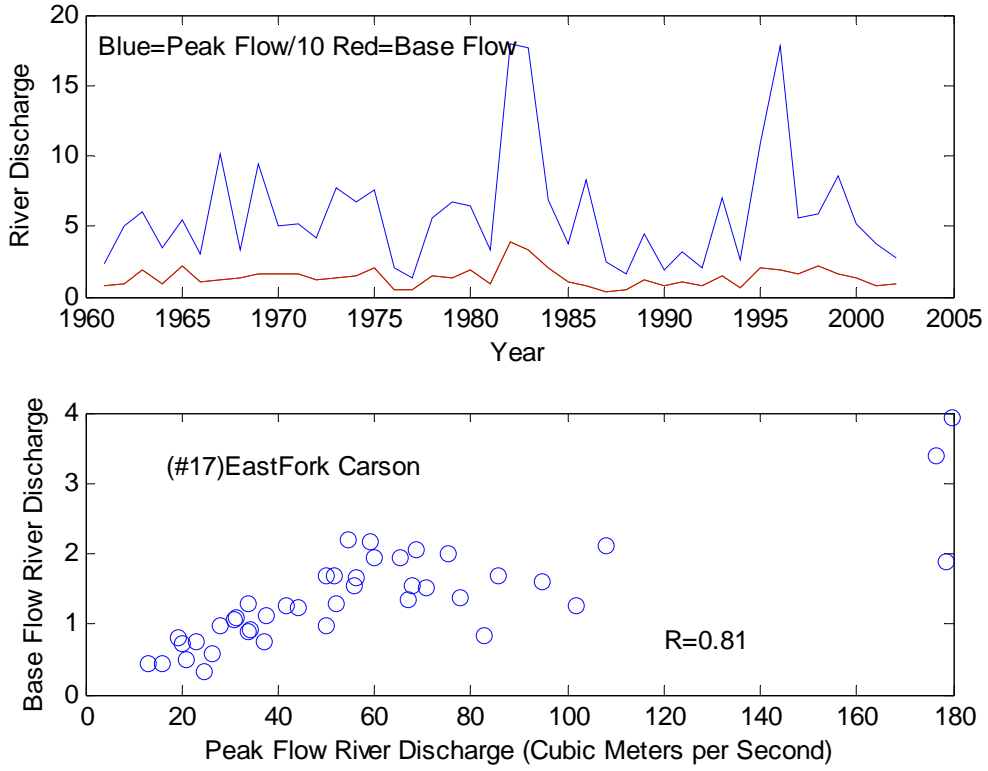


Fig. E17. Upper Panel, time series of peak flow divided by 10 (blue) and base flow (red). Lower Panel, Base flow as a linear function of peak flow.

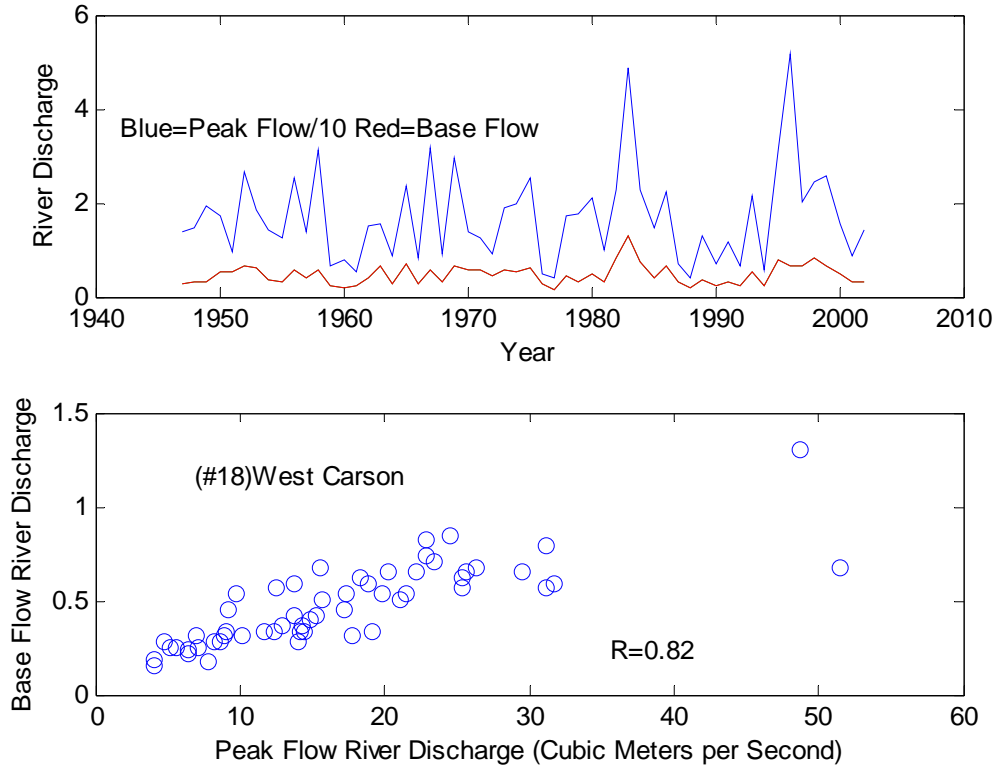


Fig. E18. Upper Panel, time series of peak flow divided by 10 (blue) and base flow (red). Lower Panel, Base flow as a linear function of peak flow.

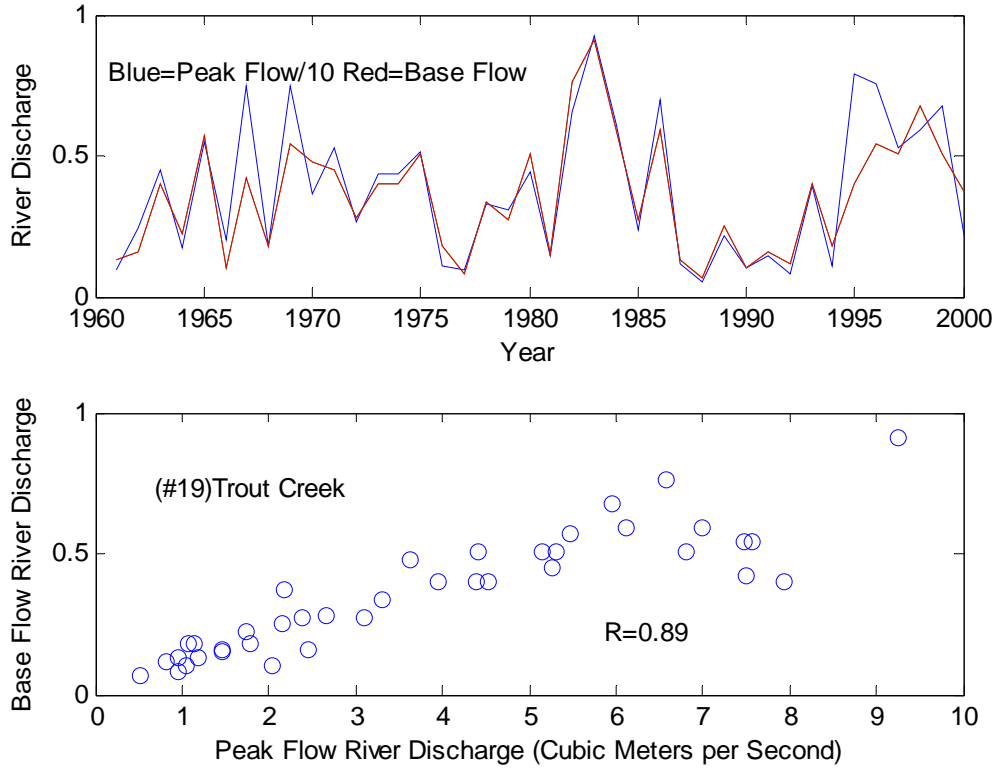


Fig. E19. Upper Panel, time series of peak flow divided by 10 (blue) and base flow (red). Lower Panel, Base flow as a linear function of peak flow. Note base flow in 1983 is higher than 1969 because 1982 was wet and 1968 was dry. The base flow Trout Creek is almost 10% of peak flow.

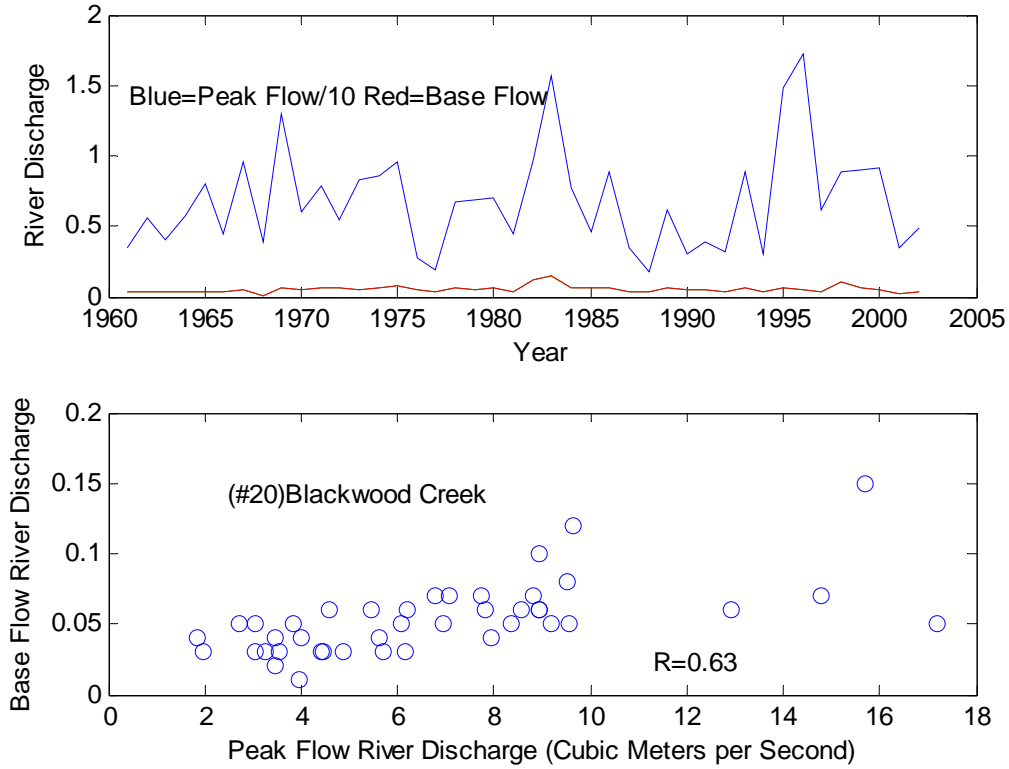


Fig. E20. Upper Panel, time series of peak flow divided by 10 (blue) and base flow (red). Lower Panel, Base flow as a linear function of peak flow.

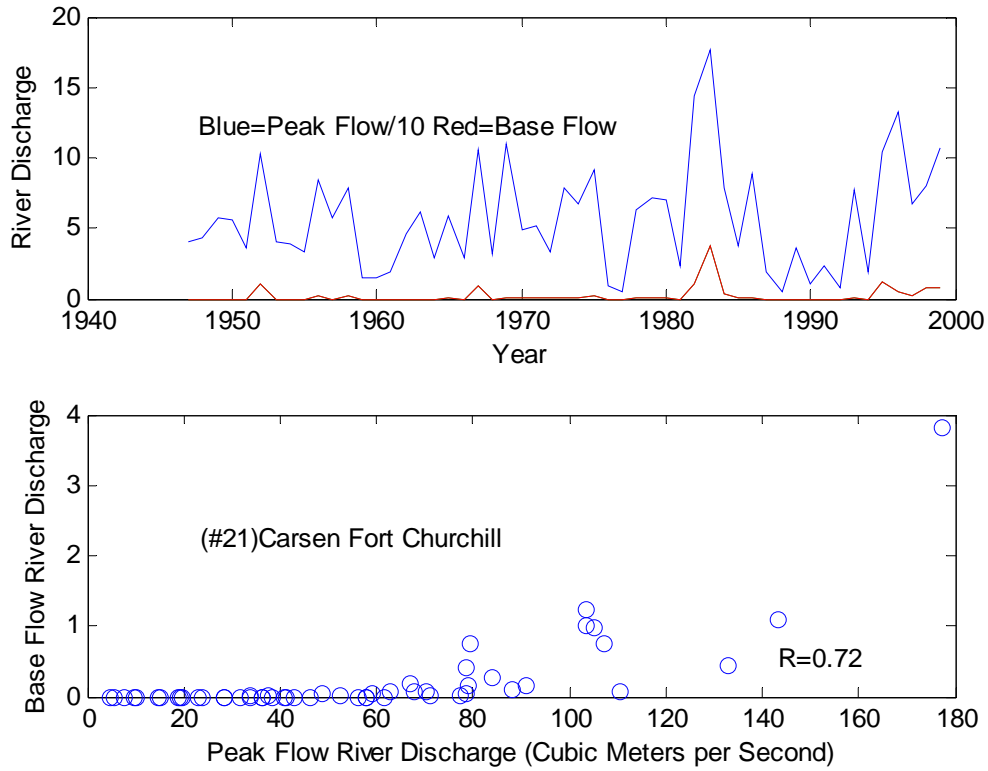


Fig. E21. Upper Panel, time series of peak flow divided by 10 (blue) and base flow (red). Lower Panel, Base flow as a linear function of peak flow. Base flow for the down stream Carson at Fort Church is probably influence by low precipitation, a low water table and upstream diversion.

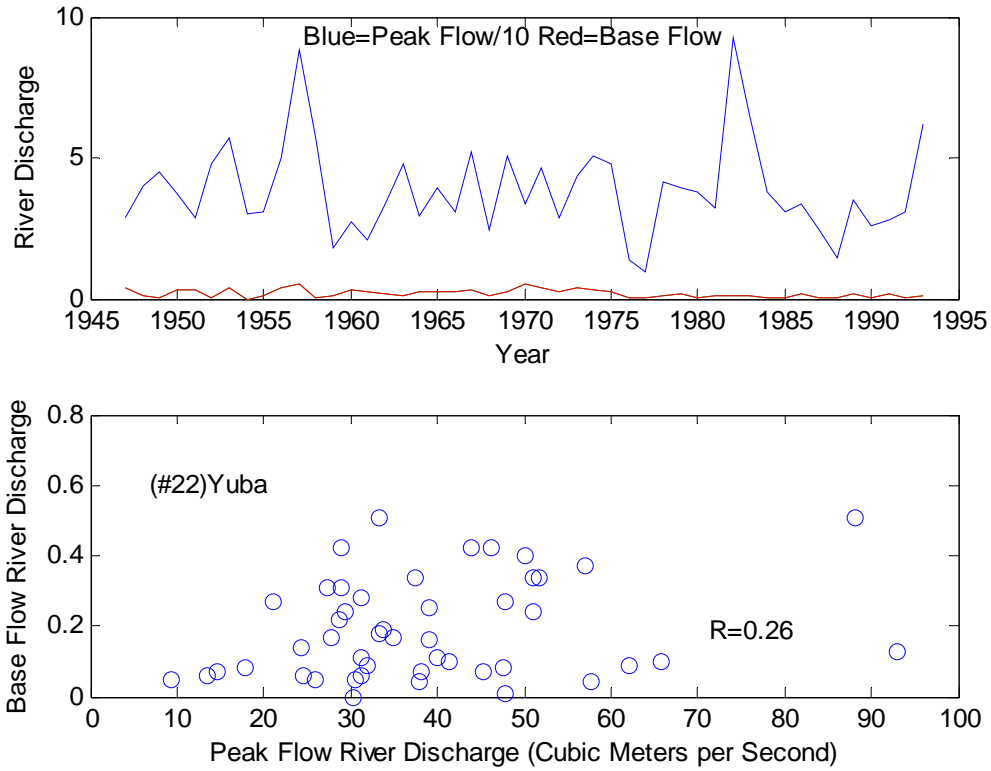


Fig. E22. Upper Panel, time series of peak flow divided by 10 (blue) and base flow (red). Lower Panel, Base flow as a linear function of peak flow.

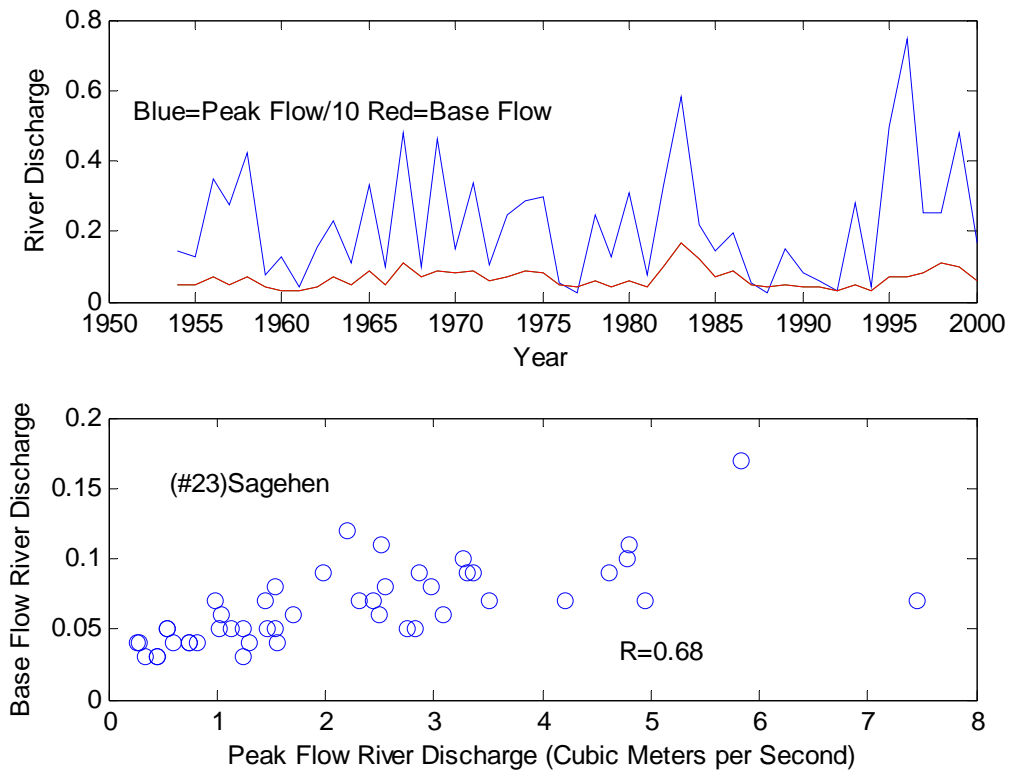


Fig. E23 Upper Panel, time series of peak flow divided by 10 (blue) and base flow (red). Lower Panel, Base flow as a linear function of peak flow.

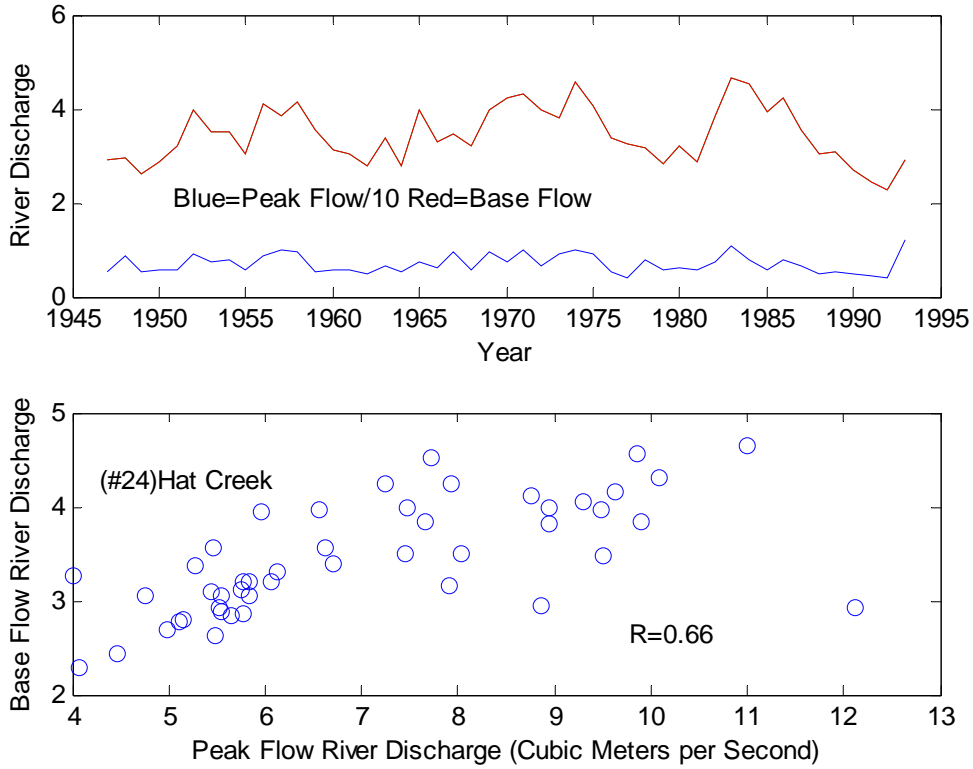


Fig. E24. Upper Panel, time series of peak flow divided by 10 (blue) and base flow (red). Lower Panel, Base flow as a linear function of peak flow. Hat Creek base flow is about 50% of peak flow and also shows the lower amplitudes and scattered correlations at higher peak flows.